INVESTIGATIONS ON CURRENT CONTROL DISTRIBUTED GENERATION SYSTEMS

A DISSERTATION SUBMITTED TOWARDS THE PARTIAL FULFILMENT OF THE REQUIREMENTS FOR THE AWARD OF THE DEGREE OF MASTER OF TECHNOLOGY IN

POWER SYSTEMS
(2010-2012)

SUBMITTED BY
Girish Gowd Talapur
Roll No. 02/PSY/2010

UNDER THE GUIDANCE OF
Dr. VISHAL VERMA

Department of Electrical Engineering
Delhi Technological University
(Formerly Delhi College of Engineering)
July 2012

Department of Electrical Engineering

Delhi Technological University

(Formerly Delhi College of Engineering)

CERTIFICATE

This is to certify that the project entitled, "**INVESTIGATIONS ON CURRENT CONTROL DISTRIBUTED GENERATION SYSTEMS**", submitted by **Mr. Girish Gowd Talapur**, University Roll No. 02/PSY/2010, student of Master of Technology (Power System) in Electrical Engineering department from Delhi Technological University (Formerly Delhi college of Engineering), is a dissertation work carried out by his under my guidance during session 2011-2012 towards the partial fulfillment of the requirements for the award of the degree of Master of Technology in Power system.

I wish his all the best in his endeavors.

Date: July 2012

Dr. VISHAL VERMA
ASSOCIATE PROFESSOR,
Electrical Engineering Department
Delhi Technological University
Shahbad daulatpur, Bawana road
Delhi- 110042.

ACKNOWLEDGEMENT

I would like to thank my honorable guide Dr. VISHAL VERMA, Associate Professor, Department of Electrical Engineering, Delhi Technological University (formerly Delhi College of Engineering). It would have never been possible for me to take this project to completion without his innovative ideas and his relentless support, encouragement and patience. I consider myself fortunate to have had a chance to work under his supervision. In spite of his hectic schedule he was always approachable and took his time o to discuss my problems and give his advice and encouragement.

I would also like to thank Dr. NARENDRA KUMAR, Head of the Department, Electrical Engineering Department, Delhi Technological University (formerly Delhi College of Engineering) for providing better facilities and constant support.

I am also very thankful to the entire faculty and staff members of the electrical engineering department and Mr. Anil Butola (Lab assistant, Simulation Lab) for their help and cooperation.

I wish to thank all my fellow students especially Shrinivas Amanchi, Ravindranath Korivi, Kranthi Mulakala, Bhawna and Renu Bhardwaj for their support throughout the project work.

I wish to thank Ph.D scholars Amritesh Kumar, ramesh singh, lovely goel, ajeet dhakar, manoj badoni and peeyush panth for the invaluable knowledge they imparted to me during course work.

Finally my greatest thank to my family and friends for their continuous support.

Date: July 2012

Girish Gowd Talapur

Roll no. 02/PSY/2010

M.tech (Power System)

ABSTRACT

Modern power system is envisaged to incorporate microgrids in the power grids to realize efficiently flexible and reliable flow of power by effectively utilizing renewable energy sources and storage systems. The microgrids is often required to operate both in grid connected and islanded mode. Typically in electrical network alternators coupled with front end transformers act as voltage source, and subject to critical control for its entry and exit from the system. Moreover, the control of these alternators is based on the reaction of the grid in terms of frequency depicting the power fluctuations and reactive power support to sustain terminal voltage constant. Such control become obvious due to rotating element in the alternator which retards the speed and in-turn the frequency of the generated supply on load, and increase for light load conditions. But Voltage Source Converters (VSCs) being static device offer no indication in frequency change upon different loading conditions. Moreover, the response of VSC is too fast, therefore, controlling it based on reaction from the grid would cause large transients.

Voltage control, identical to conventional Power System based on droop characteristics has been prescribed by many researchers, but, one due to vicinity of sources (with very low impedance between two micro sources) and estimation of power angle, there exist a large chance of circulating current which may have cascading effect. The best alternative for such micro sources in a micro grid is through current control.

This thesis investigates current control schemes for operation of micro source in grid connected and islanded mode. Typically, a master distributed generation (DG) unit and current controlled slave DGs to share the load as per their rating, and absorbs the transients arising from load perturbations and DG source switching is considered for investigation. Master DG is operated in current control while in grid connected operation and is operated with PWM switching to present a voltage source for slave DGs which are always operated in direct current control mode either under central command generating references for different DGs based on sensed voltage and by decentralized control by sensing the current at different nodes. Simulated results under MATLAB environment are presented to validate the effectiveness of the control scheme. Both load perturbations and outage of DGs is incorporated while accessing the performance evaluation of the proposed control scheme, both in grid connected and islanded mode.

Table of Contents

LIST OF FIGURES

CHAPTER 1

INTRODUCTION

1.1 General:

Power quality and high reliability for power supply to consumer is a requisition to the modern power system. Day-by-day growth in power demand has increased compulsion to increase the generation, install the new Transmission and Distribution lines to supply the increased demand and strengthen existing system. With depleting resources of fossil fuel the world is witnessing a paradigm shift for harnessing and utilizing Renewable Energy Sources (RES) and effectively utilizing them as distributed generation (DG) sources. Distributed Generation can employ both conventional and RES with storage elements. Although in abundance but the renewable energy sources like solar, wind etc, cannot be directly utilized by consumer due to various technical constraint posed by the electricity generation system utilizing these non-conventional methods. Few of such problems are varying nature both in magnitude and frequency of A.C generated by wind-turbine system, varying d.c output of solar (PV cell) system and their grid/microgrid interfaces. DG is invariably connected through power electronic converters to the grid at distributed level to supply the part of local loads demand and provide requisite power conditioning. Often several DG units employing grid tied voltage source converters (VSC) are used in parallel, forming a microgrid to satisfy the local demanded load and additionally maintains the power quality and high reliability of the supply. Microgrid is either operated in Grid connected/Islanded mode or in Standalone mode. For grid connected mode, the voltage and the frequency of the DGs are governed by utility grid, whereas in standalone or islanded operation of the microgrid the voltage and frequency is maintained locally. Storage system is invariably required in Standalone/Islanded mode to provide load matching which additionally ensure complete evacuation of generated power. In a Microgrid intelligent load sharing has to be done between parallel DGs to harness the power effectively. Different techniques are available for load sharing between parallel DGs.

1.2 Microgrids:

Microgrids are small-scale, low voltage conventional/non conventional power supply network designed to supply electricity to a small community, such as a housing estate or a suburban locality, or an academic or public community such as a university or school, a

commercial area, an industrial site, a trading estate or a municipal region. Microgrid is essentially an active distribution network because it is the conglomerate of DG systems and different loads at distribution voltage level. The distributed generators employed in a Microgrid are usually conventional/non-conventional distributed energy resources integrated together to generate power at distribution voltage. From operational point of view, the DG must be equipped with power electronic interfaces and controlled to provide the required flexibility to ensure operation as a single aggregated system and to maintain the specified power quality and energy output. This control flexibility which would allow the Microgrid to present itself to the main utility power system as a single controlled unit that meets local energy needs for reliability and security.

The key differences between a Microgrid and a conventional power plant are as follows:

i. The DGs are of much smaller capacity with respect to the large generators in conventional power plants.
ii. Power generated at distribution voltage can be directly fed to the utility distribution network.
iii. The DGs are normally installed close to the customers' premises so that the electrical loads can be efficiently supplied with satisfactory voltage and frequency profile and negligible line losses.

The technical features of a Microgrid make it suitable for supplying power to remote areas of a country where supply from the national grid system is either difficult to avail due to the network topology or frequently disrupted due to severe climatic conditions or man-made disturbances. From grid point of view, the main advantage of a Microgrid is envisaged as a controlled entity within the power system. It can be operated as a single aggregated load. This ascertains its easy controllability and compliance with grid rules and regulations without hampering the reliability and security of the power utility. From customers' point of view, Microgrids are beneficial for locally meeting their electrical requirements. They can supply uninterruptible power, improve local reliability, reduce feeder losses and provide local voltage support. From environmental point of view, Microgrids reduce environmental pollution and global warming through utilisation of low-carbon technology [1].

Microgrid Structure:

Figure.1.1 shows the basic Microgrid architecture [2]. The electrical system is considered to be radial with a collection of loads and three feeders-1, 2, and 3. The DGs are interfaced to the system through power electronics converters. The separation between the grid and the

Microgrid at the Point of Common Coupling (PCC) on the primary side of the transformer. The Microgrid must meet the prevailing interface requirements at this point, such as defined in draft standard IEEE P1547.

The sources on feeder 1 and 2 allow full examination of situations where the DGs are located away from the common feeder bus to decrease line losses, support voltage and/or use its waste heat. On a radial feeder multiple DGs increase the problem of power flow control and voltage support along the feeder when compared to all sources being located at the feeder‘s common bus. The concept used in placement of sources is based on plug-and-play concept. The distribution feeders are generally operated at 415 volts or smaller. Each microgrid has numerous circuit breakers and power and voltage controllers. The control signals to the source, regulates feeder power flow and voltage controller near each DGs. When downstream loads change then local DGs power is increased or decreased to hold the total power flow at the dispatched level.

There are two feeders with DGs and one without any generation in Figure.1.1 to show an

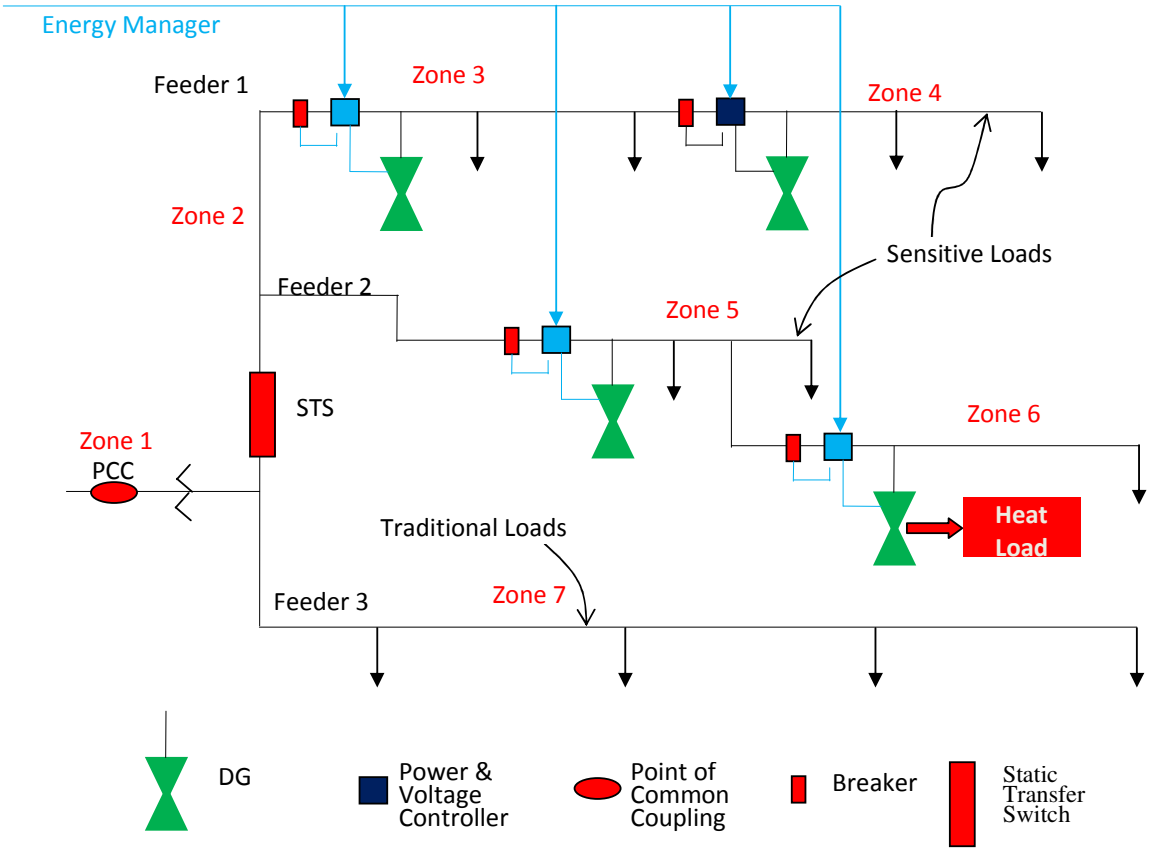

Fig.1.1: Microgrid architecture

extensive range of operation. On the bulk power system feeder 1 and 2 can island using the Static Transfer Switch (STS) during disturbances to minimize it at the sensitive loads. Islanding does not have sense if there is not sufficient power generation to meet the demands of the sensitive loads.

The Microgrid considers three critical functions that are exclusive to this architecture.

- DGs Controller: Fast responses and load changes without depending on communication which are provided by the power and voltage controller attached with DGs.
- Energy Manager: Through the dispatch of power and voltage set points to each DG it provides operational control and the time response of this function is obtained in minutes.
- Protection: In the protection of Microgrid, the sources are interfaced using power electronics and require unique solution to provide the required functionality.

i. **DGs Controller:** For the basic operation such as to regulate power flow when loads on the feeder change their operating points; regulate the voltage level at the interface of each DGs when loads changes on the system; and to insure that when the system islands each DGs rapidly picks up its shares etc. Microgrid vastly depends on the DGs Controller. Another important function of Microgrid is to island smoothly and automatically reconnect to the bulk power system. But currently available DGs does not have this set of key functions. Whole system or grid events responds in milliseconds and using the DG controller accordingly should respond further by locally measured voltage and current to control DGs. Fast communication among DGs is not necessary for Microgrid operation but it is necessary that each inverter has ability to respond to load changes in predetermined manner without getting data from other sources or locations. This prearrangement permits DGs to "plug-and-play"- i.e. changing protection and control of units are already the part of the system. The steady state set point for power 'P' and local bus voltage 'V' are the basic input to such the DGs Controller.

ii. **Energy Manager:** The Energy Manager available for system operation of the Microgrid through dispatch of power and voltage set points to each DGs Controller. This function of Energy Manager could be as simple as having a technician, who enters these set points at each controller by hands for a state-of-the-art communication system with artificial intelligence. The actual values of dispatch of P and V depending upon the operational needs of the Microgrid. Some possible criteria are:

- Insure that the necessary heat and electrical loads are met by the DGs;
- Insure that the Microgrid satisfies operational contracts with the bulk power provider;
- Minimize emissions and/or system losses; and
- Maximize the operational efficiency of the DGs.

iii. **Protection:** The protection coordinator must have ability to respond fast to both system and Microgrid faults. For a fault on the grid the protection scheme must response as fast as possible to isolate the critical load portion of the Microgrid from the grid. It has same function as an uninterruptable power supply at a potentially lower incremental cost. The response time at which the Microgrid isolates from the grid will depend on the specific customer loads on the Microgrid. In some cases to protect critical loads without separation from the distribution system sag compensation is used. When a fault occurs within islanded portion of the Microgrid the desired protection is needed to isolate the smallest possible section on the radial feeder to eliminate fault. For example a fault in Zone-4, Figure.1.1, can be find out by differential current sensing at the closest Power and Voltage Controller resulting in the operation of the nearby breaker to isolate the fault with minimum disturbances to the rest of the Microgrid.

1.3. Power Electronics Applications to Microgrids:

A power system employing wind powered turbines, fuel cell based sources, micro generators, and photovoltaic systems augmenting in the main power lines will constitute a DG system. In a DG system end users need not be passive consumers, they can be active suppliers to the grid. Conventionally, important parameters of power delivered (frequency and voltage) are monitored and controlled by the large power generator units (usually consisting of synchronous generators). In case of DG systems, the power electronic interface has to regulate the voltage, frequency, and power to link the energy source to the grid. In such environment the focus is on high power density, robust dc-ac and ac-ac modules with complex control and safety requirements [3].

WIND ENERGY SYSTEMS

Wind energy has the biggest share in the renewable energy sector. The important features associated with a wind energy conversion system are:

- Available wind energy

- Type of wind turbine employed
- Type of electric generator and power electronic circuitry employed for interfacing with the grid

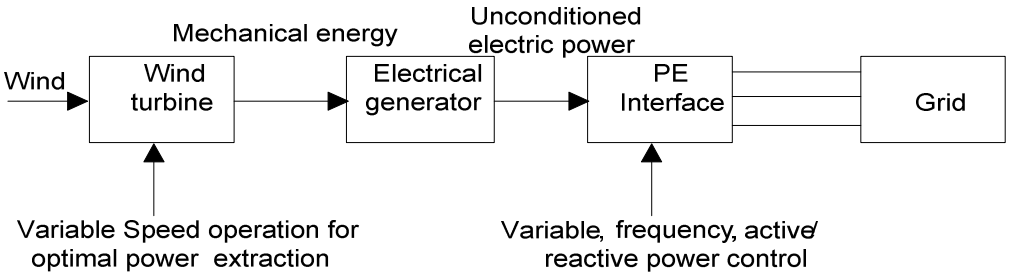

Fig.1.2: variable speed wind energy conversion system.

Fig.1.2 depicts a variable speed wind energy conversion system. The variable wind energy is converted into mechanical energy; available mechanical energy was converted into electrical energy by induction generator. But the available electrical energy is decoupled from the grid by employing a full scale ac-ac converter system, enabling a wider range of optimal operation. Such a scheme is depicted in Fig.1.3. The variable frequency ac from the turbine is fed to the three phase ac-dc-ac converter. The generator side ac-dc converter is controlled to obtain a predetermined value at the terminal of the dc link capacitor. The dc voltage is then inverted using a six-switch dc-ac inverter.

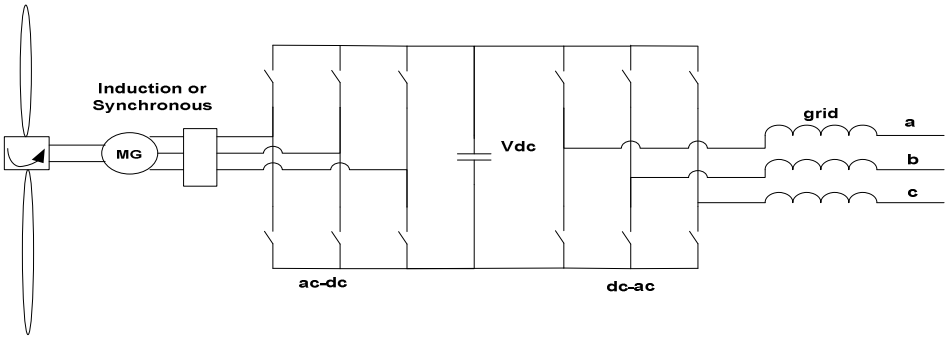

Fig.1.3: Fully variable wind energy conversion system.

FUEL CELL SYSTEMS:

The main drawbacks of fuel cells are:

- Inability to store energy - difficult to cold start
- Output voltage slowly varies with the load - requires a boost stage with regulation
- Low slew rate - hampers dynamic performance, needs backup energy storage.

Due to the above mentioned reasons, auxiliary energy storage along with PE based power conditioning is essential to realize a practical fuel cell based system. The output

voltage is low dc and in many cases line frequency ac is required (grid integration), this requires voltage step up and dc-ac inversion. To meet the dynamic load changes, energy back up (battery or ultra capacitor) is required. In Fig.1.4, the fuel cell output voltage is stepped up employing a dc-dc converter and then the stepped-up dc voltage is inverted to line frequency ac. Conventionally this method has been more popular owing to the absence of transformer and the controllability of the dc-dc converter.

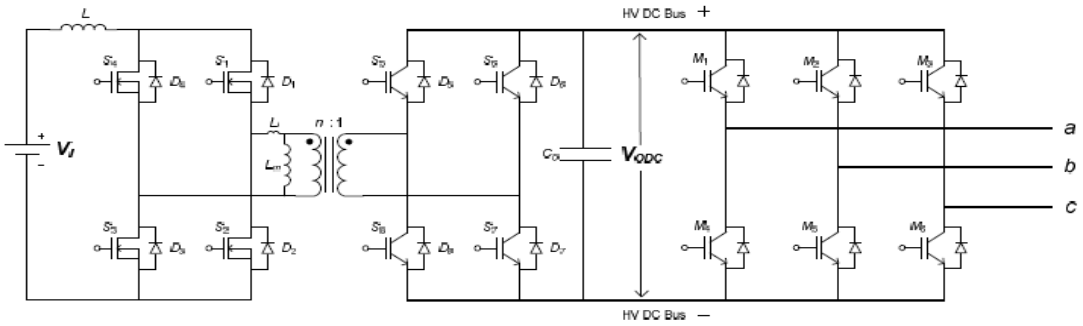

Fig.1.4: Energy conversion system with dc-dc converter followed by 3 phase VSI.

PV SYSTEM:

PV panels are formed by connecting a certain number of solar cells in series and parallel Since the cells are connected in series to build up the terminal voltage, the current flowing is decided by the weakest solar cell [4], [5]. Parallel connection of the cells would solve the low current issue but the realizing the low voltage (< 5 V). Thus the panels are connected in series and parallel to enhance the power handling ability. The entire PV system can be seen as a network of small dc energy sources with power electronics based power conditioning interfaces employed to improve the efficiency and reliability of the system.

The role of power electronics in photovoltaic's other than power conditioning is to interconnect the individual solar panels – two solar panels cannot be identical hence a dc-dc converter interfacing the two will help maintain the required current and voltage, and with regulation improve the overall efficiency.

Several non-isolated dc-dc converters have been employed for this purpose. Buck, buck-boost, boost, and Cuk topologies with suitable modifications can be employed for this purpose [5].Fig.1.5 shows a PV system with dc- dc module used to interface the PV panels.

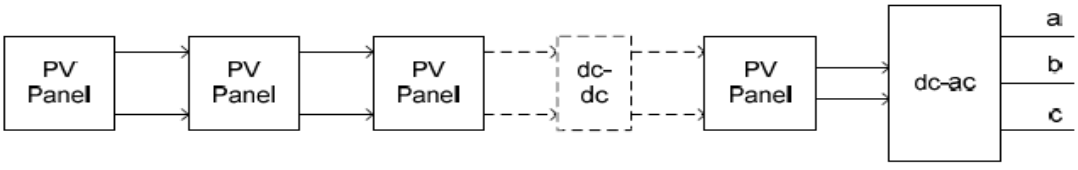

Fig.1.5: PV system with dc- dc module.

1.4. Control Strategies:

1.4.1 Synchronous and Stationary frame theory:

The αβ-frame and the dq-frame are the two main classes of two-dimensional frames. The αβ-frame enables one to transform the problem of controlling a system of three half-bridge converters to an equivalent problem of controlling two equivalent subsystems. Moreover, the concept of instantaneous reactive power been defined in the αβ-frame. The dq-frame possesses the same merits as the αβ-frame, in addition to the following:

- If the control is exercised in the dq-frame, a sinusoidal command tracking problem is transformed to an equivalent DC command tracking problem. Hence, PI compensators can be used for the control.
- In abc-frame, models of specific types of electric machine exhibit time-varying, mutually coupled inductances. If the model is expressed in dq-frame, the time varying inductances are transformed to (equivalent) constant parameters.
- Conventionally, components of large power systems are formulated and analyzed in dq-frame. Therefore, representation of VSC systems in the dq-frame enables analysis and design tasks based on methodologies that are commonly employed for power systems, in a unified framework.

1.4.2 Interactions of Microgrid with Main Grid:

When the microgrid is operating in grid connected mode, the reference voltage and the frequency for all the DGs in the microgrid are obtained by the main grid. The voltage and the frequency of the main grid are not allowed to altered by embedding appropriate control of the DGs in the microgrid. But these DGs can alter the voltage in the microgrid by supplying locally the net demand of local loads. The capacity of the microgrid is very small compared to the main grid, hence operation of the microgrid in grid connected mode does not effect the stability of the mains/grid.

In general DG units in the microgrid can operate in three ways:

i. Grid feeding unit
ii. Grid forming unit and
iii. Grid supporting unit

But whenever the microgrid is operated in grid connected mode, the DG units are operated largely as grid feeding units and grid supporting units.

1.4.3 Islanding:

For reliability concern, after a fault occurs in the distribution system (without DG units) the portion of the network located downstream from to the circuit breaker is interrupted by the circuit breaker followed by a number of operations driven by the control centre to restore supply at all the load points. The presence of DG affects the system reliability in different ways, both by introducing an additional source of failures, and by taking advantage of the presence of the local generators in order to speed up the service restoration after permanent faults, by analysing the possible formation of islands during the service restoration process.

The islanding issue is the main concern in the participation of DG to the service restoration process. Islanding refers to the condition when portions of the distribution system are only supplied only from microgrid, with some distinctions:

i. non-intentional islanding occurs if after the fault it is not possible to disconnect the microgrid; non-intentional islands must then be detected and eliminated as fast as possible;
ii. intentional islanding refers to the formation of islands of predetermined or variable extension; these islands have to be supplied from suitable sources able to guarantee acceptable voltage support and frequency, controllability and quality of the supply, and may play a significant role in assisting the service restoration process;

After a fault in the distribution system, the microgrid is switched off to avoid their negative impact on the fault currents and on the action of the protection systems. Hence, the loads inside the island experience a momentary interruption. If the microgrid is connected to the grid through a static device, its contribution to the short current is relatively low and the momentary interruption could be avoided. However, if the microgrid is unable to sustain the island, it has to be switched off as fast as possible. The DG unit in microgrid should be able to follow the load during and after the island formation and its circuit breaker must be able to identify the fault currents to avoid the wrong island reconnection when a fault occurs inside the island.

Once the island is formed, automatic reconnection of the island without proper resynchronisation has to be avoided. After the service restoration, the connection to the island is closed only if there is nearly perfect synchronism. Synchronisation is performed by means of a suitable control system, with voltage and phase regulation available inside the island.

1.4.4 Load sharing:

The load sharing between DGs are somewhat different than in conventional power system, conventional power system as changes in load demand is automatically shared by the alternators according their capacities which in turn alters the frequency the voltage of system. But in microgrid, all DGs are act as constant frequency sources, which are insensitive change in frequency to overloading/under loading, and the poor voltage regulation is marred by deficit/surplus of both real and reactive power in the microgrid. The demarcation in real/reactive power need is done by determining the real and reactive components of current drawn by the net connected loads, and then intelligent load sharing has to be done between the DGs to fulfil the overload condition and reactive VARs supplied for voltage regulation. Different load sharing techniques are available for parallel operation of DGs, they are

i. Droop method
ii. Master-Slave method
iii. Average load sharing method

1.4.5 Power Conditioning:

The utility is concerned due to the high penetration level of intermittent RES in distribution systems as it may pose a threat to network in terms of stability, voltage regulation and power-quality (PQ) issues. Therefore, the DG systems are required to comply with strict technical and regulatory frameworks to ensure safe, reliable and efficient operation of overall network. With the advancement in power electronics and digital control technology, the DG systems can now be actively controlled to enhance the system operation with improved PQ at PCC. However, the extensive use of power electronics based equipment and non-linear loads at PCC generate harmonic currents, which may deteriorate the quality of power.

Generally, current controlled voltage source inverters are used to interface the intermittent RES in distributed system. Recently, a few control strategies for grid connected inverters incorporating PQ solution have been proposed. An inverter operates as active inductor at a certain frequency to absorb the harmonic current. But the exact calculation of network inductance in real-time is difficult and may deteriorate the control performance. A similar approach in which a shunt active filter acts as active conductance to damp out the harmonics in distribution network. In [6], a control strategy for renewable interfacing inverter based on - theory is proposed. In this strategy both load and inverter current sensing is required to compensate the load current harmonics.

The non-linear load current harmonics may result in voltage harmonics and can create a serious PQ problem in the power system network. Active power filters (APF) are extensively used to compensate the load current harmonics and load unbalance at distribution level. This results in an additional hardware cost. However, in this paper authors have incorporated the features of APF in the, conventional inverter interfacing renewable with the grid, without any additional hardware cost. Here, the main idea is the maximum utilization of inverter rating which is most of the time underutilized due to intermittent nature of RES. It is shown in this paper that the grid-interfacing inverter can effectively be utilized to perform following important functions:

1) Transfer of active power harvested from the renewable resources (wind, solar, etc.);

2) Load reactive power demand support;

3) Current harmonics compensation at PCC; and

4) Current unbalance and neutral current compensation in case of 3-phase 4-wire system. Moreover, with adequate control of grid-interfacing inverter, all the four objectives can be accomplished either individually or simultaneously. The PQ constraints at the PCC can therefore be strictly maintained within the utility standards without additional hardware cost.

1.5 FUTURE SCOPE:

Operation of microgrid is accepted by researchers around the globe and currently seen the hot topic for exploration. Various aspects are investigated as discussed aforesaid. Substantial efforts an still a requisite to study the operation of the grid coupling realized by voltage source converter for determining the individual contributions of power in the network microgrid while its operation in grid coupled mode and islanded mode. The challenge lies in accurate estimation of reference commands that control the VSC for power flow into/out of the microgrid by the individual DG units. The control needs to keep a clear cut vigil on transients arising of switching of loads and DGs moving in/out of microgrids. The operation also include detection of islanding and operation of microgrid under off grid operation, controlling the DGs fast to take up the load dynamics and manage storage systems adequately so that none of DG should go out of step to reinitiate/replan load matching for the off grid operation. Maintenance of PQ issue becomes prime under off grid mode due to system reflecting as a weak system, and proliferation of PQ problems seriously affect the operation of other DGs and sensitive loads.

CHAPTER-2

Literature Survey

2.1. General:

Incorporation of renewable energy sources into the grid is the highly popular subject now-a-days, since fossile fuels are fast depleting and there is a thrust on clean and green environment friendly technologies for power generation and consumption. The best possible way to include RES in the generation capacity is through their grid coupling in the form of micro grids. The proper operation of microgrids in both grid coupled and off grid mode may reap the benefits of the effective and efficient utilization of RES. A micro grid may constitute of several, variety of RES sources with different dynamics, capacities, sensitivity and output types, where their inclusion in the grid need to be interfaced with VSCs. The operation of VSC in coherence with different VSCs in a micro gird is a distinct challenge particularly while dealing with loads sharing, transients handling, management of generated power, faster control of power flow, cost effective topologies and control elements together with power quality improvements on the grid, etc. In this chapter, a comprehensive introductive survey for different control technologies, connection configuring/topologies and operational control in both grid coupled and isolated mode are described.

2.2. Reviews of Literature:

A large number of publications have appeared in the field of distributed generation, operation of micro grids, detection of islanding conditions, voltage and current control of VSCs, centralized and decentralized control of DGs with simulation results and experimented results (for small systems in off grid mode).

The concept of micro grid has introduced in twenty first century where emphasis has been laid on usage of RES, and the need for their effective utilization with grid storage. Their operation is majorly seen in parity with conventional sources having alternators which operate in coherence with other alternators controlling the power based on frequency control. The responses of alternators are slow and dependent on the inertia of their respective rotor shafts. The overloading is observed by fall in frequency. Even though VSCs do not have any rotating part and generally operate with fixed frequency in response to load perturbations, they are operated with droop characteristics P/f and Q/V. And, each DG is separately seen as voltage source controlled by PWM signals to generate sinusoid at set value of voltage magnitude and phase. Some investigations is also reported to visualize the microgrid having

DGs connecting to the grid as a current source, while one of the source act as master in off grid applications. Different control for synchronizing and estimation of control command is also reported for fast operation of DGs, together with power quality improvements and load sharing. A detailed summary of literature is presented in the subsequent sections of the chapter in following sequence.

(i) Synchronizing and estimation of reference signals.

(ii) Operation in grid coupled and islanded needs.

(iii) Power sharing between DGs.

2.2.1. Synchronizing and estimation of reference signals

Correct estimation of reference signals for proper synchronization of DG with microgrid is as prerequisite for effective control. Any deviation from exact reference may lead to circulation of dangerously high level of circulating currents which may jeopardize the operation of microgrid. The estimation has to be very fast so as to apply the control in real time, thus frequency domain techniques will certainly not apply. Various time domain techniques, viz, IRPT, SRF synchronous detection technique, symmetrical components technique, etc. are reported in the literatures for realizing a fast control. SRF based technique is seen as suitable most and hence witnessed wide acceptance due to its insensitivity to operation amidst distorted and unbalanced voltages in the microgrid. However, SRF technique demands a fast PLL which should provide the synchronizing sine and cosine signals. The detailed survey of the literature is presented in the following sub sections:

2.2.1.1. Synchronous Reference Frame Control:

Synchronous reference frame control, also called dq control, uses a reference frame transformation module, e.g., abc → dq, to transform the grid current and voltage waveforms into a reference frame that rotates synchronously with the grid voltage. By means of this, the control variables become dc values; thus, filtering and controlling can be easier achieved [7]. A schematic of the dq control is represented in Fig. 2.1.

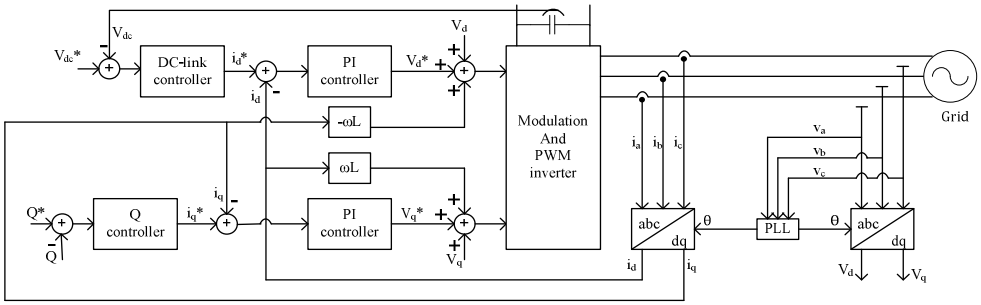

Fig.2.1 General structure for synchronous rotating frame control structure.

In this structure, the dc-link voltage is controlled in accordance to the necessary output power. Its output is the reference for the active current controller, whereas the reference for the reactive current is usually set to zero, if the reactive power control is not allowed. In the case when the reactive power is controlled, a reactive power reference must be imposed to the system. The dq control structure is normally associated with proportional–integral (PI) controllers since they have a satisfactory behaviour when regulating dc variables. The matrix transfer function of the controller in dq coordinates can be written as

$$G_{PI}^{(dq)}(s) = \begin{bmatrix} K_p + \frac{K_i}{s} & 0 \\ 0 & K_p + \frac{K_i}{s} \end{bmatrix} \quad (2.1)$$

where K_p is the proportional gain and K_i is the integral gain of the controller.

Since the controlled current has to be in phase with the grid voltage, the phase angle used by the abc → dq transformation module is extracted from the grid voltages. As a solution, filtering of the grid voltages and using arctangent function to extract the phase angle is an effective possibility [8]–[10]. In addition, the phase-locked loop (PLL) technique is now a state of the art technique in extracting the phase angle of the grid voltages in the case of distributed generation systems.For improving the performance of PI controller in such a structure as depicted in Fig. 2.1, cross-coupling terms and voltage feed forward are usually used [7], [11], [12]. In other cases, with all these improvements, the compensation capability of the low-order harmonics in the case of PI controllers is very poor, standing as a major drawback when used in grid connected systems.

2.2.1.2. Stationary Reference Frame Control:

Another possible way to structure the control loops is to use the implementation in stationary reference frame, as shown in Fig. 2.2.

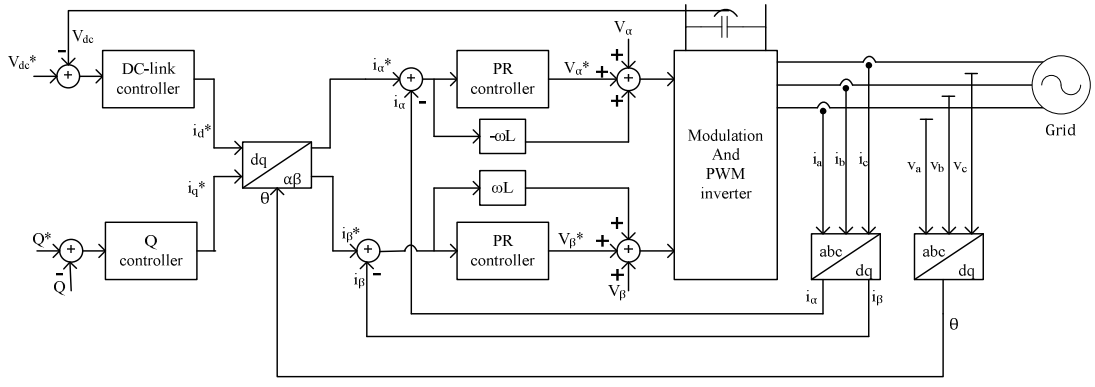

Fig.2.2 General structure for stationary reference frame control strategy.

In this case, the grid currents are transformed into stationary reference frame using the abc → αβ module. Since the control variables are sinusoidal in this situation and due to the known drawback of PI controller in failing to remove the steady-state error when controlling sinusoidal waveforms, employment of other controller types is necessary. Proportional resonant (PR) controller [13]–[16] gained a large popularity in the last decade in current regulation of grid-tied systems.

In the PR case, the controller matrix in the stationary reference frame is given by

$$G_{PR}^{(\alpha\beta)}(s) = \begin{bmatrix} K_p + \frac{K_i s}{s^2+\omega^2} & 0 \\ 0 & K_p + \frac{K_i s}{s^2+\omega^2} \end{bmatrix} \quad (2.2)$$

where ω is the resonance frequency of the controller, K_p is the proportional gain, and K_i is the integral gain of the controller.

Characteristic to this controller is the fact that it achieves a very high gain around the resonance frequency, thus being capable to eliminate the steady-state error between the controlled signal and its reference [15]. The width of the frequency band around the resonance point depends on the integral time constant Ki. A low Ki leads to a very narrow band, whereas a high Ki leads to a wider band. Moreover, high dynamic characteristics of PR controller are reported in variety of applications [16].

2.2.2. Grid coupling

In all grid-connected converters such as the static VAR compensators, active power filters, and grid-connected distributed generation (DG) systems, a phase-detecting technique provides a reference phase signal synchronized with the grid voltage that is required to control and meet the power quality standards. This is particularly critical in converter-interfaced DG units where the synchronization scheme should provide a high degree of immunity and insensitivity to power system disturbances, harmonics, unbalances, voltage sags, and other types of pollution that exist in the grid signal [17]–[19]. An ideal synchronization scheme must 1) proficiently detect the phase angle of the utility signal, 2) smoothly track the phase and frequency variations, and 3) forcefully reject harmonics and disturbances. These factors, together with implementation simplicity and cost, are all important when examining the credibility of a synchronization scheme.

[20] presents a new synchronization method that demonstrates not only an advanced synchronization performance in a corrupted grid environment but also effectively handles the unbalanced situations. The technique does not require a synchronizing tool such as PLL, and its main building block is a modified adaptive notch filter (ANF) system of nonlinear

dynamical equations for real-time extraction and measurement of harmonics and reactive components of a power signal of a time-varying characteristic. The adaptive nature of the aforesaid technique allows perfect tracking of frequency and amplitude variations.

2.2.3. Islanding

During abnormal conditions and failure of grid, the microgrid usually disconnects itself and supports locally the connected load, such phenomenon is referred to Islanding. Large number of issues is needed to be addressed by the microgrid by fast control action on load matching, detecting the islanding not the transient etc. Following such section deals with such a aforesaid issue [21].

2.2.3.1. ISSUES WITH ISLANDING:

Although there are some benefits of islanded operation and there are some drawbacks as well. Some of them are as follows:

- Line worker safety can be threatened by DG sources feeding a system after primary sources have been opened and tagged out.
- The voltage and frequency may not be maintained within a standard permissible level.
- The islanded system may be inadequately grounded by the DG interconnection.
- Instantaneous reclosing could result in out of phase reclosing of DG. As a result of which large mechanical torques and currents are created that can damage the generators or prime movers [22]. Also, transients are created, which are potentially damaging to utility and other customer equipment. Out of phase reclosing, if occurs at a voltage peak, will generate a very severe capacitive switching transient and in a lightly damped system, the crest over-voltage can approach three times rated voltage [23].

Due to these reasons, it is very important to detect the islanding quickly and accurately.

2.2.3.2. ISLANDING DETECTION

The main philosophy of detecting an islanding situation is to monitor the DG output parameters and/or system parameters and decide whether or not an islanding situation has occurred from change in these parameters. Islanding detection techniques can be divided into remote and local techniques and local techniques can further be divided into passive, active and hybrid techniques as shown in Figure 2.3.

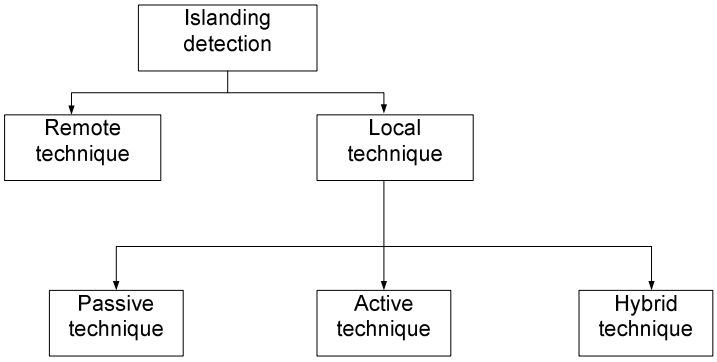

Fig 2.3: Islanding detection techniques.

A. Remote Islanding Detection Techniques

Remote islanding detection techniques are based on communication between utilities and DGs. Although these techniques may have better reliability than local techniques, they are expensive to implement and hence uneconomical. Some of the remote islanding detection techniques are as follows:

Transfer trip scheme: The basic idea of transfer trip scheme is to monitor the status of all the circuit breakers and reclosers that could island a distribution system. Supervisory Control and Data Acquisition (SCADA) systems can be used for that [24]. This method requires a better interaction between the utility and DGs and this often increases the costs for both the utility and DG owners.

Power line signaling scheme: Here, a signal generator at the transmission system continuously broadcasts a signal to the distribution feeders using the power line as the signal path. DGs are equipped with signal receivers. If the receiver does not sense the signal (caused by the opening of breakers between the transmission and distribution systems), there is an island condition [25]. Figure 2.4 shows a power line signaling scheme. This scheme can be effectively used in multi DG system.

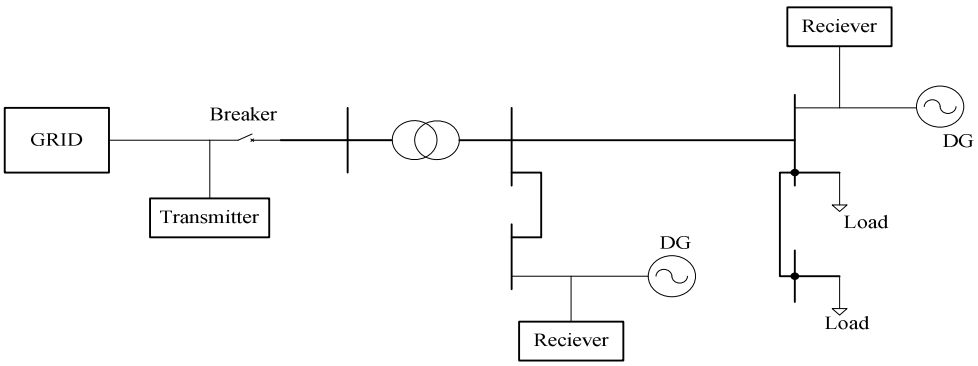

Fig 2.4: A power line signalling scheme

B. Local Detection Techniques

It is based on the measurement of system parameters at the DG site, like voltage, frequency, etc. It is further classified as:

i. Passive detection techniques:

Passive methods work on measuring system parameters such as variations in voltage, frequency, harmonic distortion, etc. These parameters vary greatly when the system is islanded. Differentiation between an islanding and grid connected condition is based upon the thresholds set for these parameters. Special care should be taken while setting the threshold value so as to differentiate islanding from other disturbances in the system. Passive techniques are fast and they don't introduce disturbance in the system but they have a large non detectable zone (NDZ) where they fail to detect the islanding condition. There are various passive islanding detection techniques and some of them are as follows:

Rate of change of output power: The rate of change of output power, dP/dt , at the DG side, once it is islanded, will be much greater than that of the rate of change of output power before the DG is islanded for the same rate of load change [24]. It has been found that this method is much more effective when the distribution system with DG has unbalanced load rather than balanced load [26].

Rate of change of frequency: The rate of change of frequency, df/dt , will be very high when the DG is islanded. The rate of change of frequency (ROCOF) can be given by [27]

$$\text{ROCOF}, \frac{df}{dt} = \frac{\Delta P}{2HG} f$$

Where, ΔP is power mismatch at the DG side

H is the moment of inertia for DG/system

G is the rated generation capacity of the DG/system

Large systems have large H and G where as small systems have small H and G giving larger value for df/dt . ROCOF relay monitors the voltage waveform and will operate if ROCOF is higher than setting for certain duration of time. The setting has to be chosen in such a way that the relay will trigger for island condition but not for load changes. This method is highly reliable when there is large mismatch in power but it fails to operate if DG's capacity matches with its local loads. However, an advantage of this method along with the rate of change of power algorithm is that, even they fail to operate when load matches DG's generation, any subsequent local load change would generally lead to islanding being detected as a result of load and generation mismatch in the islanded system.

Rate of change of frequency over power: df/dP in a small generation system is larger than that of the power system with larger capacity. Rate of change of frequency over power utilize this concept to determine islanding condition. Furthermore, test results have shown that for a small power mismatch between the DG and local loads, rate of change of frequency over power is much more sensitive than rate of change of frequency over time [28].

Change of impedance: The utility impedance is considerably smaller than the impedance of a power island. The impedance of a section of network will increase when that section becomes disconnected from the utility [29]. Continuous monitoring the source impedance will give the idea of whether the system is islanded or not. Voltage unbalance: Once the islanding occurs, DG has to take charge of the loads in the island. If the change in loading is large, then islanding conditions are easily detected by monitoring several parameters: voltage magnitude, phase displacement, and frequency change. However, these methods may not be effective if the changes are small. As the distribution networks generally include single-phase loads, it is highly possible that the islanding will change the load balance of DG. Furthermore, even though the change in DG loads is small, voltage unbalance will occur due to the change in network condition [30].

Harmonic distortion: Change in the amount and configuration of load might result in different harmonic currents in the network, especially when the system has inverter based DGs. One approach to detect islanding is to monitor the change of total harmonic distortion (THD) of the terminal voltage at the DG before and after the island is formed [31]. The change in the third harmonic of the DG's voltage also gives a good picture of when the DG is islanded [32].

ii. Active detection techniques

With active methods, islanding can be detected even under the perfect match of generation and load, which is not possible in case of the passive detection schemes. Active methods directly interact with the power system operation by introducing perturbations. The idea of an active detection method is that this small perturbation will result in a significant change in system parameters when the DG is islanded, whereas the change will be negligible when the DG is connected to the grid. Some of the active detection techniques are as follows:

Reactive power export error detection: In this scheme, DG generates a level of reactive power flow at the point of common coupling (PCC) between the DG site and grid [27] or at the point where the Reed relay is connected. This power flow can only be maintained when the grid is connected. Islanding can be detected if the level of reactive power flow is not maintained at the set value. For the synchronous generator based DG, islanding can be

detected by increasing the internal induced voltage of DG by a small amount from time to time and monitoring the change in voltage and reactive power at the terminal where DG is connected to the distribution system. A large change in the terminal voltage, with the reactive power remaining almost unchanged, indicates islanding [33]. The major drawbacks of this method are it is slow and it cannot be used in the system where DG has to generate power at unity power factor.

Impedance measurement method: The main philosophy is the same as that of the passive technique that the impedance of the system changes with islanding. In an active direct method, a shunt inductor is briefly connected across the supply voltage time to time and the short circuit current and supply voltage reduction is used to calculate the power system source impedance [27]. However, in an indirect method, a high frequency signal is injected on the DG terminal through a voltage divider. This high frequency signal becomes more significant after the grid is disconnected [29].

Phase (or frequency) shift methods: Measurement of the relative phase shift can give a good idea of when the inverter based DG is islanded. A small perturbation is introduced in form of phase shift. When the DG is grid connected, the frequency will be stabilized. When the system is islanded, the perturbation will result in significant change in frequency. The Slip-Mode Frequency Shift Algorithm (SMS) [34] uses positive feedback which changes phase angle of the current of the inverter with respect to the deviation of frequency at the PCC. A SMS curve is given by the equation:

$$\theta = \theta_m \sin\left(\frac{\pi}{2}\frac{(f^{(k-1)}-f_n)}{(f_m-f_n)}\right) \qquad (2.3)$$

Where θ_m is the maximum phase shift that occurs at frequency f_m. f_n is the nominal frequency and $f^{(k-1)}$ is the frequency at previous cycle. A SMS curve is designed in such a way that its slope is greater than that of the phase of the load in the unstable region [21]. When the utility is disconnected, operation will move through the unstable region towards a stable operating point. Islanding is detected when the inverter frequency exceeds the setting.

This detection scheme can be used in a system with more than one inverter based DG. The drawback of this method is that the islanding can go undetected if the slope of the phase of the load is higher than that of the SMS line, as there can be stable operating points within the unstable zone [35].

Active Frequency Drift (AFD): is reported by adding a short period of zero time in the output current of the inverter based DG [21]. T_I and T_V are the time period for a half cycle of DG's output current and utility voltage, respectively. T_Z , dead or zero time, is the time for

which the DG's output current remains zero. When such distorted waveform is applied and there is no grid connection, the voltage frequency of the islanded system will shift up or down continuously as the inverter operating at unity power factor tends to seek the resonant frequency of the local load. This method is very effective for purely resistive loads but it may fail for other loads [36].

iii. Hybrid detection schemes

Hybrid methods employ both the active and passive detection techniques. The active technique is implemented only when the islanding is suspected by the passive technique. Some of the hybrid techniques are discussed as follows:

Technique based on positive feedback (PF) and voltage imbalance (VU): This islanding detection technique uses the PF (active technique) and VU (passive technique) [37]. The main idea is to monitor the three-phase voltages continuously to determinate VU which is given as

$$VU = \frac{V_{+Sq}}{V_{-Sq}} \tag{2.4}$$

V_{+Sq} and V_{-Sq} are the positive and negative sequence voltages, respectively. Voltage spikes will be observed for load change, islanding, switching action, etc. Whenever a VU spike is above the set value, frequency set point of the DG is changed. The system frequency will change if the DG has been islanded.

Technique based on voltage and reactive power shift: In this technique voltage variation over a time is measured to get a covariance value (passive) which is used to initiate an active islanding detection technique, adaptive reactive power shift (ARPS) algorithm [38].

$$\text{Co-variance } (T_{av'}, T_v) = E\left(T_{av'}^{(n)} - U_{av}\right)\left(T_v^{(n)} - U_v\right) \tag{2.5}$$

Where,

$T_{av'}$ is the average of the previous four voltage periods.

U_{av} is the mean of $T_{av'}$

T_v is the voltage periods

U_v is the mean of T_v

It also uses the d-axis current shift instead of current phase shift. The d-axis current shift, i_d^k , or reactive power shift is given as

$$i_d^k = k_d \left(\frac{T_{av'} - T_v^{(k)}}{T_v^{(k)}}\right) \tag{2.6}$$

k_d is chosen such that the d-axis current variation is less than 1 percent of q-axis current in inverter's normal operation. The additional d-axis current, after the suspicion of island, would

accelerates the phase shift action, which leads to a fast frequency shift when the DG is islanded.

2.2.4. Load sharing

2.2.4.1. Master-slave control techniques

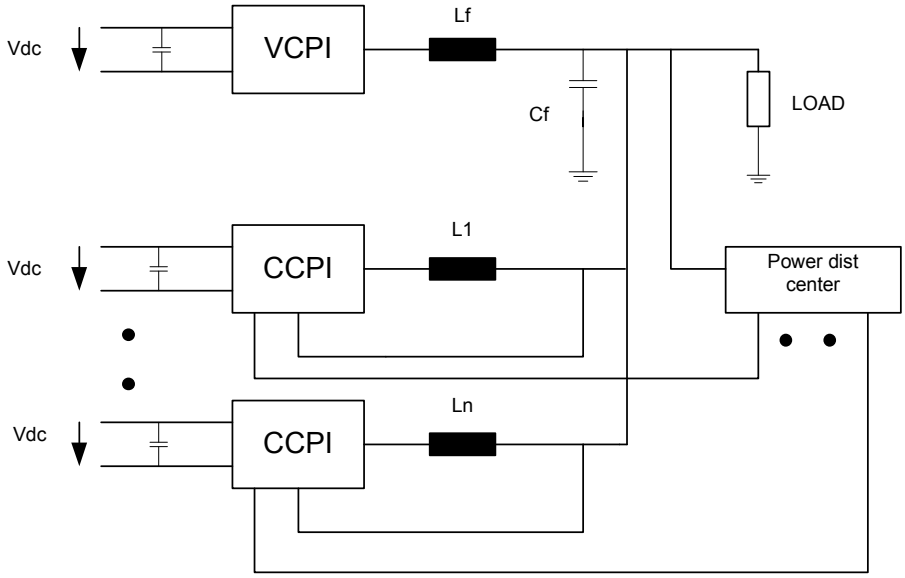

Fig 2.5: Combined voltage- and current-controlled inverters [41].

The master/slave control method uses a voltage-controlled inverter as a master unit and current-controlled inverters as the slave units. The master unit maintains the output voltage sinusoidal, and generates proper current commands for the slave units [39, 40].

One of the master/slave configuration is the scheme suggested in [41,42], is shown in Fig.2.5, which is a combination of voltage-controlled and current-controlled PWM inverters for parallel operation of a single phase uninterruptible power supply (UPS). The types of PWM inverters considered are voltage-controlled (VCPI) or current controlled (CCPI) with voltage source. The voltage-controlled inverter (master) is developed to keep a constant sinusoidal wave output voltage. The current-controlled inverter units are operated as slave controlled to track the distributive current. The inverters do not need a phased locked loop (PLL) circuit for synchronization since these units are interlinked and are communicating with the power centre (A PLL is needed when the frequency is measured from the grid such as in the droop method where it is the only way of communicating, or if the inverter have only to supply power to the grid and is not part of the control scheme as solar inverters current application); this gives a good load sharing. However, the system is not redundant since it has a single point of failure.

In [43] the paper focus on operation and behaviour of the isolated microgrids under different conditions and scenarios. This was investigated for two main control strategies, single master operation where a voltage source inverter (VSI) can be used as voltage reference (grid forming) when the main power supply is lost; all the other inverters can then be operated in PQ mode (grid supporting). And multi-master operation where more than one inverter are operated as a VSI, other PQ inverters may also coexist.

In more recent papers [44,45] an enhanced approach is introduced, the master inverter is replaced by a central control block which controls the output voltages and can influence the output current of the different units, this is sometimes called central mode control or distributed control. This means that the voltage magnitude, frequency and power sharing are controlled centrally (commands are distributed through a low-bandwidth communication channels to the inverters) and other issues such as harmonic suppression are done locally.

2.2.4.2. Current/power sharing control techniques

In this control technique the total load current is measured and divided by the number of units in the system to obtain the averaged unit current. The actual current from each unit is measured and the difference from the average value is calculated to generate the control signal for the load sharing [39].

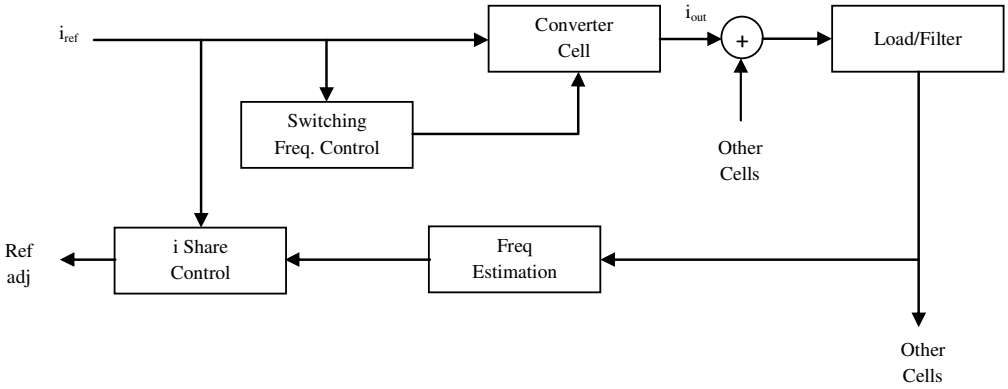

Fig 2.6: Proposed current sharing control in [46, 47].

A method of current sharing for paralleled power converters is introduced and then explored in [46, 47], and the block diagram is shown in Fig.2.6. Each converter is controlled such that their average output current is directly related to its switching frequency. As a result, the frequency content of the aggregate output ripple voltage contains information about the individual cell output currents. Each cell measures the output ripple voltage and uses this information to achieve current balance with the other cells.

The authors in [48] proposed an inverter current feed-forward compensation which makes the output impedance resistive rather than inductive in order to get a precise load sharing. In [49] solution is proposed to compensate the harmonic circulating currents due to PWM non-synchronization and in turn affects the load sharing precision. The digital control is done in [50] for parallel connected three-phase inverters. The algorithm include high-speed current control as a minor loop which offer low voltage distortion even for nonlinear loads. In [51] the focus is shown on developing a solution for the DC offset between paralleled inverters and its effect on the circulating currents. In [52] the authors suggested two-line shared bus connecting all inverters, one for current sharing control and the other to adjust the voltage reference.

2.2.4.3. Frequency and voltage droop control techniques:

Many methods found in the literature can be roughly categorized into the following:

i) Adopting a conventional frequency/voltage droop control.

ii) Opposite frequency/voltage droop control.

iii) Droop control in combination with other methods.

i) Adopting a conventional frequency/voltage droop control:

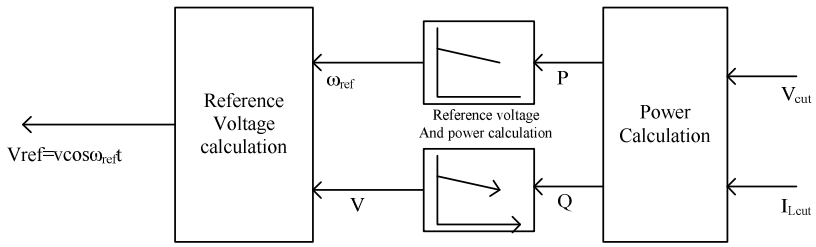

Fig 2.7: Reference voltage and power calculation [53].

In [53] a control technique is proposed for operating two or more single-phase inverter modules in parallel with no auxiliary interconnections. An inner current loop and an outer voltage loop controls, is prescribed for each module as shown in Fig.2.7. This technique is similar to the conventional frequency/voltage droop concept using frequency and fundamental voltage droop to allow all independent inverters to share the load in proportion to their capacities.

In [54] scheme for controlling parallel connected inverters in a stand-alone ac supply system is presented and control scheme is depicted in Fig.2.8. This scheme is suitable for control of inverters in distributed source environments such as in isolated AC systems,

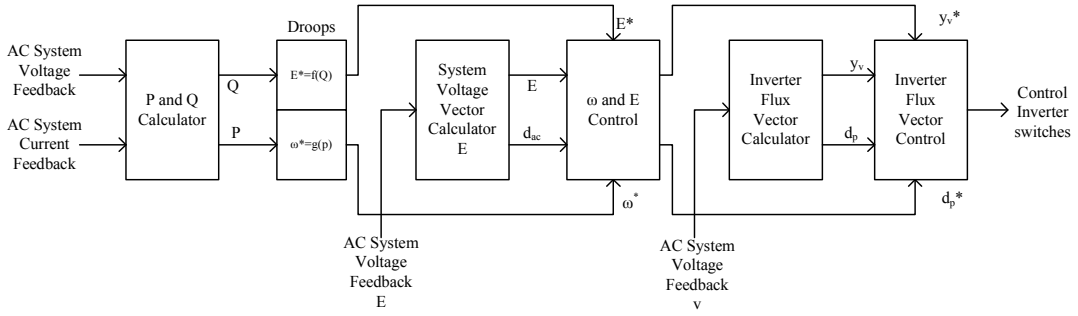

Fig 2.8: Inverter control scheme [54].

large UPS systems, and PV systems connected to AC grids. Active and reactive power sharing between inverters can be achieved by controlling the power angle (by means of frequency), and the fundamental inverter voltage magnitude. The look-up table implementation is dealt in [55]. However, the inductance connected between the inverter and the load makes the output impedance high. Therefore, the voltage regulation as well as the voltage waveform quality is not good under load change conditions as well as nonlinear load condition. The authors explain the same concept but with focusing in control issues of UPS systems in [56].

In [57] an interesting autonomous load sharing technique for parallel connected three-phase voltage source converters is presented. This paper focuses on an improvement to the conventional frequency droop scheme for real power sharing and the development of a new reactive power sharing scheme. The improved frequency droop scheme computes and sets the phase angle of the VSC instead of its frequency. It allows the operator to tune the real power sharing controller to achieve desired system response without compromising frequency regulation by adding an integral gain into the real power control. The proposed reactive power sharing scheme introduces integral control of the load bus voltage, combined with a reference that is drooped against reactive power output. This causes two VSCs on a common load bus to share the reactive load exactly in the presence of mismatched interface inductors if the line impedances are much smaller than the interface reactors (assuming short lines).

In [58] the authors are considering that large DC cross currents can flow between the different inverters which is normally neglected since only the AC cross current is normally taken into consideration by means of control schemes. However, this can happen only if we have a considerable DC voltage offset difference between the inverters which is usually not the case since these errors are generated by the sensors and they are very small. One more condition to make this happen is a very small output resistance of each inverter in comparison to it is output impedance. It should be noted that this droop scheme can only make inverters

have the same DC-offset voltage so as to avoid the DC cross current, whereas it cannot get rid of the DC-offset voltage.

In [59–61] the author discuss the application of conventional droops for voltage source inverters and categorize the system components to form a modular AC-hybrid power system. Then, in [62] by the same author an investigation is carried out what is called "opposite droop" (active power/voltage and reactive power droop) control is reported. The embedded discussion focused on the need of different droop functions for different types of grids. In [62] it is found that for high voltage (mainly inductive lines) grids the regular droop functions can be used, whereas, for low voltage (mainly resistive) grids, so-called opposite droop functions should be used instead. The case off regular droop functions is advantageous since it allows connectivity to higher voltage levels and power sharing with rotating generators [62–65].

A microgrid control was introduced and implemented in [66–68], the microgrid has two critical components, the static switch and the micro-source. The static switch has the ability to autonomously island the microgrid from disturbances such as faults, events described in IEEE 1547, or power quality events. After islanding, the reconnection of the microgrid is achieved autonomously after the tripping event is no longer present. This synchronization is achieved by using the frequency difference between the islanded microgrid and the utility grid insuring a transient free operation without having to match frequency and phase angles at the connection point. Each micro-source can seamlessly balance the power on the islanded microgrid using a power vs. frequency droop controller. This frequency droop also insures that the microgrid frequency is different from the grid to facilitate reconnection to the utility.

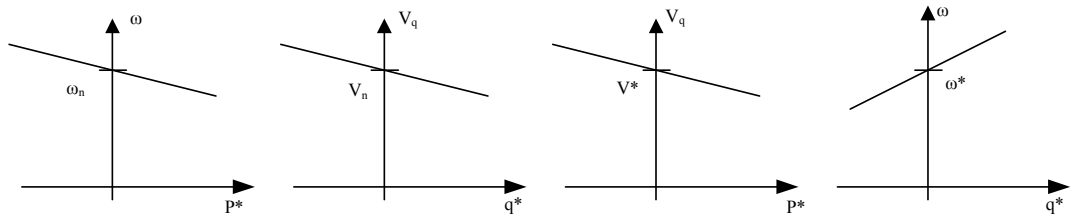

Fig 2.9: Regular conventional droop functions (left) and transient droop functions (right) [63, 70].

ii) Opposite frequency/voltage droop control

In [63,70] modified droop functions for inverters are reported in distributed generation systems so that the regular droop functions are used in the steady-state case and opposite droops are used in transients, see Fig.2.9. The steady-state droop functions are according to:

$$p_s^* = K_\omega(\omega_{ref} - \omega)$$

$$q_s^* = K_v\left(v_{ref} - v_q\right)$$

where p_s and q_s are the active and reactive power references. For the transient droop functions droop functions according to:

$$v_s^* = K_v\left(v_{ref} - v_q\right)$$

$$q_s^* = K_\omega\left(\omega_{ref} - \omega\right)$$

Where $\omega_{ref} = \omega^*$ and $v_{ref} = v^*$.

For line inductance in the same order of magnitude as the converter output filter inductance, there can be a considerable degradation of power quality in terms of voltage disturbance. The origin of this degradation is the LC-circuit formed by the line inductance and the converter AC side capacitors. Furthermore, using this approach it is not possible to connect with the high level voltage which is using the regular conventional droop functions.

In [70–74] the author focused on the transient behaviour of parallel connected UPS inverters, and it is claimed that damping and oscillatory phenomena of phase shift difference between the paralleled inverters could cause instabilities, and a large transient circulating current may occur that can overload and damage the paralleled inverters. To overcome this they proposed "droop/boost" control scheme which adds integral-derivative terms to the droop function to realize stable steady-state for frequency and phase and a good dynamic response. The method has not taken into consideration if the distance between the inverters, which is normally ease in distributed generation, where an inductive impedance component appears between each mode. Nevertheless, when an inverter is connected in such circumstances suddenly to the common AC bus, a current peak appears due to the initial phase error [75].

Compatibility problems are expected because of the opposite droop scheme. The characteristic and the scheme are shown below (Fig.2.10):

$$E = E^* - nP - n_d\frac{dP}{dt}$$

$$\omega = \omega^* - mQ - m_d\frac{dQ}{dt}$$

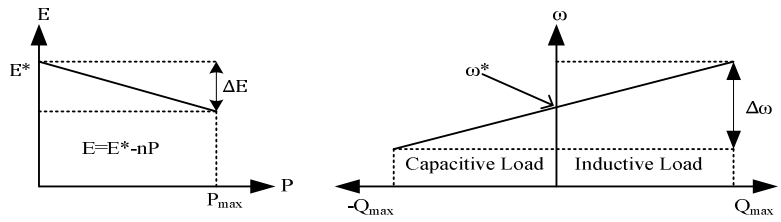

Fig 2.10: Static droop/boost characteristics for resistive output impedance [70–74].

As an addition in [69] a soft-start is included to avoid the initial current peak as well as a bank of band pass filters in order to share the significant output current harmonics. In more recent papers [76, 77] the authors use the conventional droop equations for a Microgrid too.

$$E = E^* - n(Q - Q^*)$$

$$\omega = \omega^* - m(P - P^*)$$

In [78–80] each inverter supplies a current that is the result of the voltage difference between a reference AC voltage source and the grid voltage across a virtual impedance with real and/or imaginary parts. The reference AC voltage source is synchronized with the grid, with a phase shift, depending on the difference between nominal and real grid frequency. This method behaviour is equal to the normal existing droop control methods except that, short-circuit behaviour is better since it is controlling the active and reactive currents and not the power. Its behaviour is also better in case of a non-negligible line resistance. The emulation of the finite-output impedance is obtained by the use of a hybrid voltage–current controller. Instead of having a current-control-loop inside a voltage-control-loop (or the other way round), both current and voltage are simultaneously controlled to emulate the finite-output impedance. Here, the linear quadratic Gaussian (LQG) optimal control approach is reported, using a Kalman estimator and a linear quadratic regulator as shown in Fig.2.11.

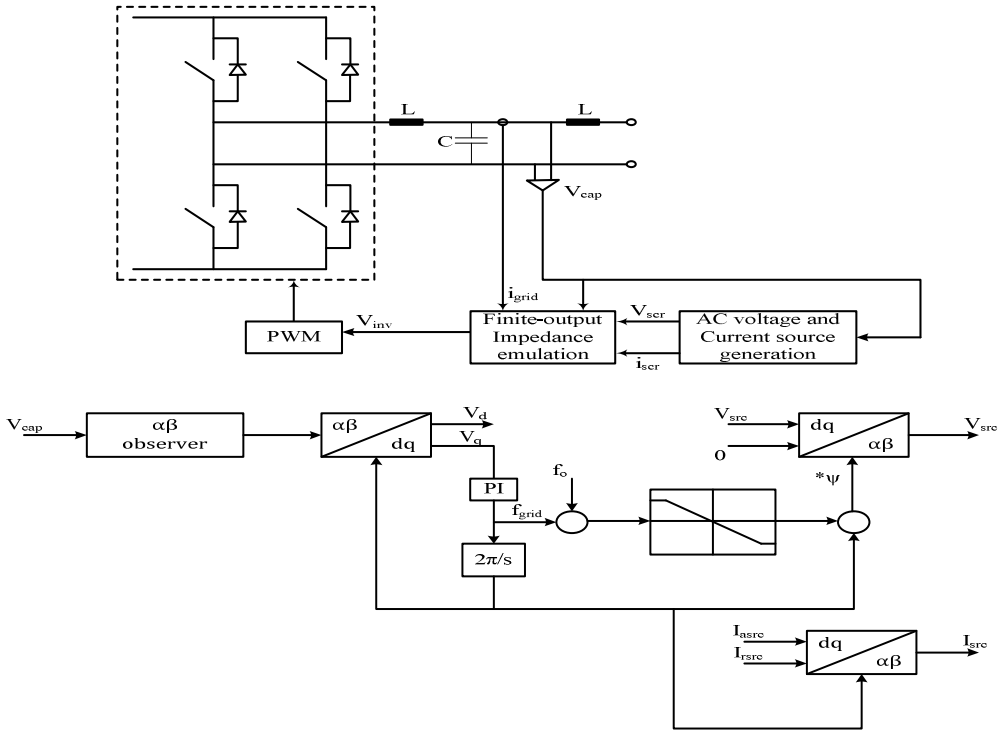

Fig 2.11: Overall scheme for the proposed droop control method (top) and the full scheme of the generation source (bottom).

The author of [81] discussed the problem of inverters with very low output impedance (such as those employing resonant controllers) directly connected in parallel through a near zero impedance cable. Low THD content and good current sharing are simultaneously obtained by controlling the load angle through an least mean square (LMS) estimator and by synthesizing a variable inductance in series with the output impedance of the inverter, while the harmonic current sharing is achieved by controlling the gain of the resonant controllers at the selected frequencies.

In [82, 83] the proposed droop scheme for UPS inverters is shown below, see Fig.2.12, in which the inverter connects with the load via series impedance (Z) like the conventional approach. However, there exist two differences.

i) The series impedance is created by the inverter internally, no true impedance is required. As a result, the inverters connect with the load tightly.
ii) The series impedance is frequency-dependent; it exhibits a reactive characteristic at the fundamental frequency and a resistive characteristic at the harmonic frequency. This means that the current sharing and voltage regulation is effective for both linear load and nonlinear load, and the performance is insensitive to parameter mismatch of the inverters.

In [84-86] the reported control method used low-bandwidth data communication signals between each generation system in addition to the locally measurable feedback signals. The focus is on systems of distributed resources that can switch from grid connection to island operation without causing problems for critical loads. This is shown achieved by combining two control methods: droop control method and average power control method. In this method, the sharing of real and reactive powers between the units is implemented by two independent control variables: power angle and inverter output voltage amplitude.

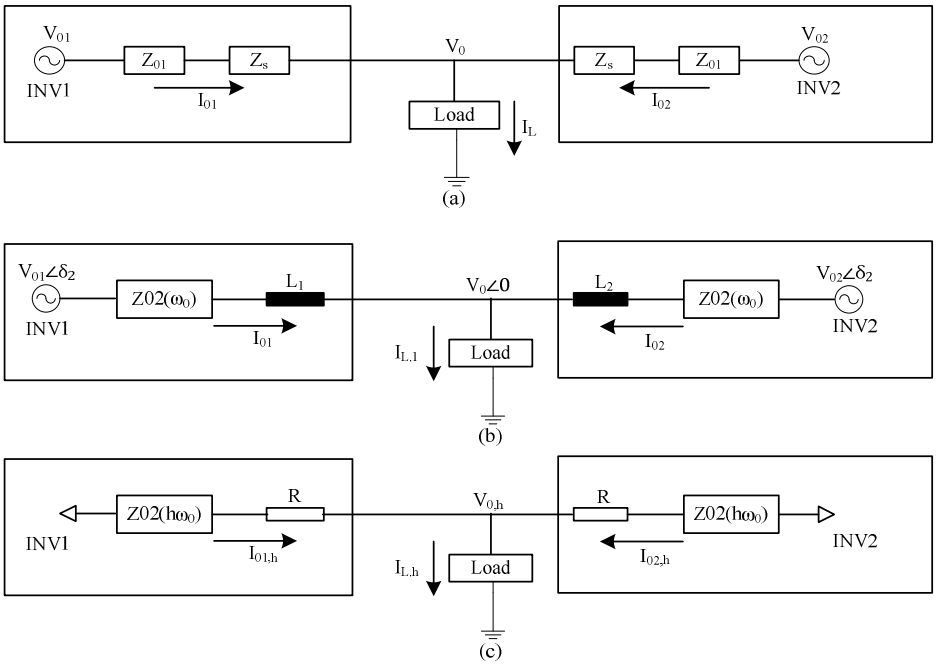

Fig 2.12: Frequency-dependent droop scheme: (a) the series impedance is created in the inverter internally; (b) the equivalent inverter circuit at the fundamental frequency and (c) the equivalent inverter circuit at the harmonic frequency [82, 83].

CHAPTER-3

Modelling and Control Theory

3.1 GENERAL

An accurate and simple modeling of an electrical system is a prerequisite as it enables engineers and researches to get an insight of the system. The system behavior and dynamics can be observed in mathematical equation. In this chapter a mathematical model of the proposed system is presented to address the concerns mentioned above. This mathematical model has simple equation which can be solved as per the system requirement. We cannot work directly to the real system because we do not know the behavior and dynamics of system. How behaves it's in transient condition and also do not know the stability of the system in transient condition. Without the modeling of the system we may get the unpredictable result and condition that's why we need the modeling of the system.

3.2 MODELING OF SYSTEM

Fig.3.1 illustrates a circuit model of VSC feeding through Δ/*Y* transformer emulating the DGS studied in this chapter, and each such DGS model consists of a DC voltage source, a three-phase PWM inverter, an *L–C* output filter, a Δ/*Y* transformer, and a load. of course, a DC voltage source may come from one of various generation sources: combustion engine, small hydro, photovoltaic arrays, fuel cells, micro-turbines, or battery energy storage systems.

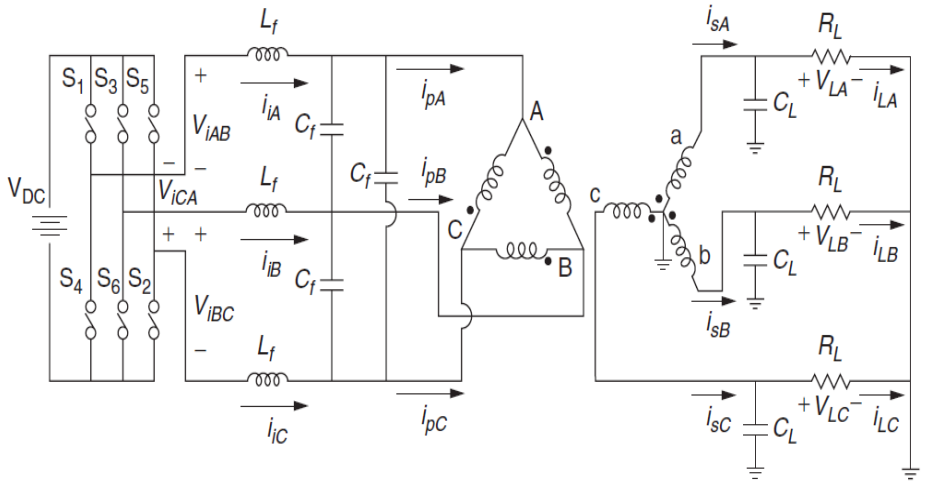

Fig.3.1 Each DGS Circuit Model.

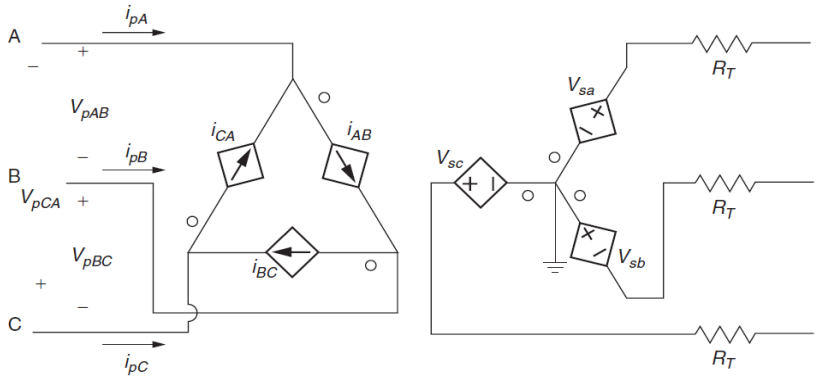

Fig.3.2: Δ/*Y* Transformer Model.

Particularly, the three-phase (Δ/*Y* type) transformer is further modelled using a controlled voltage source, a controlled current source, and equivalent phase impedances with the resistorR_T and the inductor L_T as shown in Fig. 3.2. The power rating of each transformer is 150 kVA, and turn ratio between the primary side (*Np*) and secondary side (*Ns*) is 11000:415. The primary side and secondary side voltages are 11kv (RMS, line to line) and 415 (RMS, line to line), respectively. The circuit system defined in Figs. 3.1 and 3.2 uses the following quantities to describe its behavior. The inverter output line-to-line voltage is represented by the vector $V_i = [V_{iAB} \quad V_{iBC} \quad V_{iCA}]^T$. The three-phase inverter output currents are i_{iA}, i_{iB}, and i_{iC} . Based on these currents, a vector can be defined as$I_i = [i_{iAB} \quad i_{iBC} \quad i_{iCA}]^T$ $I_i = [i_{iA} - i_{iB} \quad i_{iB} - i_{iC} \quad i_{iC} - i_{iA}]^T$. The transformer primary side line-to-line voltage is represented by the vector $V_p = [V_{pAB} \quad V_{pBC} \quad V_{pCA}]^T$.The transformer primary side is Δ connected and the line current vector is defined as$I_p = [I_{pA} \quad I_{pB} \quad I_{pC}]^T$. The transformer secondary side is *Y* connected and the phase voltage and current vectors are represented by $V_s = [V_{sa} \quad V_{sb} \quad V_{sc}]^T$and $I_s = [I_{sa} \quad I_{sb} \quad I_{sc}]^T$, respectively. At the output terminal, the load voltage and current vectors can be represented by $V_L = [V_{La} \quad V_{Lb} \quad V_{Lc}]^TandI_l = [I_{la} \quad I_{lb} \quad I_{lc}]^T$, respectively. The three phase (Δ/*Y* type) transformer has *Np* turns in the primary side windings and *Ns* turns in the secondary side windings. Based on Fig. 3.2, the voltage relation between the two sides of the transformer can be described by [87]

$$V_{sa} = \frac{N_s}{N_p} V_{pAB}\,, \qquad V_{sb} = \frac{N_s}{N_p} V_{pBC}\,, \qquad V_{sc} = \frac{N_s}{N_p} V_{pCA}\,. \qquad (3.1)$$

similarly, the current relation is

$$i_{AB} = \frac{N_s}{N_p} i_{sa}\,, \qquad i_{BC} = \frac{N_s}{N_p} i_{sb}\,, \qquad i_{CA} = \frac{N_s}{N_p} i_{sc}\,. \qquad (3.2)$$

From Fig. 3.2, it also can be observed that

$$i_{pA} = i_{AB} - i_{CA}\,,\ i_{pB} = i_{BC} - i_{AB}\,,\ i_{pC} = i_{BA} - i_{BC}\,. \tag{3.3}$$

On the primary side of the transformer, the *L–C* filter yields the following current equations:

$$\begin{aligned} i_{iA} + C_f \frac{dV_{pCA}}{dt} &= C_f \frac{dV_{pAB}}{dt} + i_{pA}\,, \\ i_{iB} + C_f \frac{dV_{pAB}}{dt} &= C_f \frac{dV_{pBC}}{dt} + i_{pB} \\ i_{iC} + C_f \frac{dV_{pBC}}{dt} &= C_f \frac{dV_{pCA}}{dt} + i_{pC}\,. \end{aligned} \tag{3.4}$$

From Eqs. (3.2)–(3.4), it is easy to derive

$$\begin{aligned} \frac{dV_{pAB}}{dt} &= \frac{i_{iAB}}{3C_f} + \frac{1}{3C_f}\frac{N_s}{N_p}(2i_{sa} - i_{sb} - i_{sc}), \\ \frac{dV_{pBC}}{dt} &= \frac{i_{iBC}}{3C_f} + \frac{1}{3C_f}\frac{N_s}{N_p}(-i_{sa} + 2i_{sb} - i_{sc}), \\ \frac{dV_{pCA}}{dt} &= \frac{i_{iCA}}{3C_f} + \frac{1}{3C_f}\frac{N_s}{N_p}(-i_{sa} - i_{sb} + 2i_{sc}). \end{aligned} \tag{3.5}$$

Rewrite Eq. (3.5) into matrix form:

$$\frac{dV_p}{dt} = \frac{1}{3C_f} I_i - \frac{1}{3C_f} T_i I_s\,, \tag{3.6}$$

Where

$$T_i = \frac{N_s}{N_p}\begin{bmatrix} 2 & -1 & -1 \\ -1 & 2 & -1 \\ -1 & -1 & 2 \end{bmatrix} \tag{3.7}$$

Equation (3.1) can be rewritten as

$$V_s = \begin{bmatrix} V_{sa} \\ V_{sb} \\ V_{sc} \end{bmatrix} = \frac{N_s}{N_p}\begin{bmatrix} 1 & 0 & 0 \\ 1 & 0 & 0 \\ 0 & 0 & 1 \end{bmatrix}\begin{bmatrix} V_{pAB} \\ V_{pBC} \\ V_{pCA} \end{bmatrix} = T_v V_p\,. \tag{3.8}$$

It is easy to write the *L–C* filter voltage equations as follows:

$$\begin{aligned} L_f \frac{di_{iA}}{dt} - L_f \frac{di_{iB}}{dt} &= V_{iAB} - V_{pAB}\,, \\ L_f \frac{di_{iB}}{dt} - L_f \frac{di_{iC}}{dt} &= V_{iBC} - V_{pBC}\,, \\ L_f \frac{di_{iC}}{dt} - L_f \frac{di_{iA}}{dt} &= V_{iCA} - V_{pCA}\,. \end{aligned} \tag{3.9}$$

Rewrite Eq. (3.9) into matrix form:

$$\frac{dI_i}{dt} = \frac{1}{L_f} V_i - \frac{1}{L_f} V_p. \tag{3.10}$$

The load current equation can be written as

$$\frac{dV_L}{dt} = \frac{1}{C_L} I_s - \frac{1}{C_L} I_L. \tag{3.11}$$

The voltage equation of the secondary side circuit is

$$\frac{dI_s}{dt} = -\frac{R_T}{L_T} I_s - \frac{1}{L_T} T_v V_p - \frac{1}{L_T} V_L \,. \tag{3.12}$$

Equations (3.6), (3.10), (3.11), and (3.12) are the four state equations for each DGS circuit model or, say, the control plant of the proposed feedback system in this chapter. The state variables of the system are V_p, I_i , V_L , and I_s , the control input is the inverter output line-to-line voltage V_i, and the disturbance is the load current I_L .

The three-phase system represented by the above state space model can be transformed from the *abc* reference frame into stationary *qd*0 reference frame using Eq. (3.13).

$$f_{qd0} = K_s f_{abc} \tag{3.13}$$

Where

$$K_s = \frac{2}{3}\begin{bmatrix} 1 & -1/2 & -1/2 \\ 0 & -\sqrt{3}/2 & \sqrt{3}/2 \\ 1/2 & 1/2 & 1/2 \end{bmatrix}, \quad f_{qd0} = [f_q \quad f_d \quad f_0]^T, \quad f_{abc} = [f_a \quad f_b \quad f_c]^T,$$

and *f* denotes either a voltage or a current variable.,

Rewrite the previous state equations [(3.6), (3.10)–(3.12)] into the stationary *qd*0 reference frame defined above:

$$\frac{dV_{pqd}}{dt} = \frac{1}{3C_f} I_{iqd} - \frac{1}{3C_f} T_{iqd0} I_{sqd0}\,, \tag{3.14}$$

$$\frac{dI_{iqd}}{dt} = \frac{1}{L_f} V_{iqd} - \frac{1}{L_f} V_{pqd}. \tag{3.15}$$

$$\frac{dV_{Lqd0}}{dt} = \frac{1}{C_L} I_{sqd0} - \frac{1}{C_L} I_{Lqd0}. \tag{3.16}$$

$$\frac{dI_{sqd0}}{dt} = -\frac{R_T}{L_T} I_{sqd0} - \frac{1}{L_T} T_{vqd0} V_{pqd} - \frac{1}{L_T} V_{Lqd0}\,. \tag{3.17}$$

Where

$$T_{iqd0} = [K_s \quad T_i \quad K_s^{-1}]_{row\ 1,2} = \frac{N_s}{N_p}\frac{3}{2}\begin{bmatrix} 2 & 0 & 0 \\ 0 & 2 & 0 \end{bmatrix}$$

and

$$T_{vqd0} = [K_s \quad T_v \quad K_s^{-1}]_{col\ 1,2} = \frac{N_s}{N_p}\begin{bmatrix} 1 & 0 \\ 0 & 1 \\ 0 & 0 \end{bmatrix}.$$

All the above vectors with qd subscriptions are two dimensional vectors where the zero sequence elements are not included. Because the transformer is Δ/Y type with the neutral point of the secondary side grounded, the secondary side circuit may carry unbalanced three-phase current (e.g., load unbalanced fault can cause zero sequence current). The transient behavior of the zero sequence circuit is uncontrollable in that the circuit is not accessible for the control inputs V_{iq} and V_{id} .

3.3 GRID SYNCHRONIZATION

In our work distributed generation systems can operate in both islanding or grid connected mode, when main grid is disconnected from main grid than microgrid goes in islanding (autonomous) mode and distributed generation systems operated in voltage control mode from current controlled mode . To ensure a smooth re-connection of the microgrid back to the main grid when the grid recovers from a fault, a microgrid re-synchronization method is also required. When the main is back on, the microgrid has been operating in the islanding mode and has its own PCC terminal voltage magnitude, frequency and phase angle, which most likely are different from those at the main grid terminal. A re-synchronization scheme is thus needed before closing the separation switch. The resynchronization is to ensure the voltage magnitude, frequency and phase angle at the microgrid end and main grid end match for a smooth reconnection of the two systems.

3.3.1 Prevalent Techniques of Phase Locked Loop

PLL structures can be broadly classified into the following categories.

Zero Crossing Detection (ZCD):

In this PLL, the phase angle is detected by synchronizing the PLL rotating reference frame and the utility voltage vector. Setting the direct axis reference voltage (Vd*) to zero results in the lock in of the PLL output on the phase angle of the utility voltage vector. In addition, the instantaneous frequency and amplitude of the voltage vector are also determined. The feed forward frequency command is introduced to improve the overall tracking performance of the PLL. The tuning of the feedback gains requires the determination of an equivalent linear model,

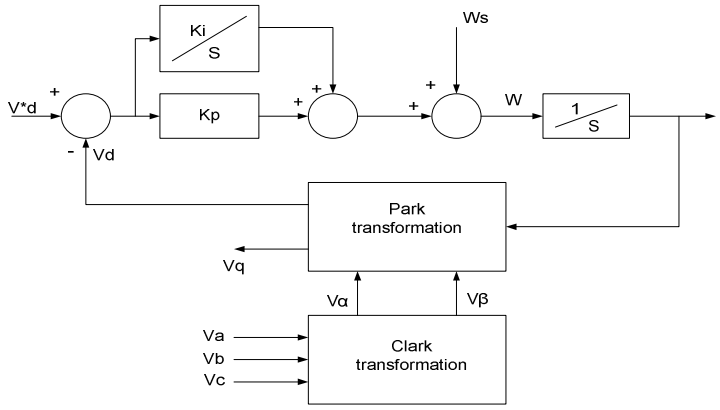

Fig.3.3: Three-Phase PLL Structure

shown in Fig.3.4. From this small signal model, one can derive the state space representation of the three-phase PLL topology.

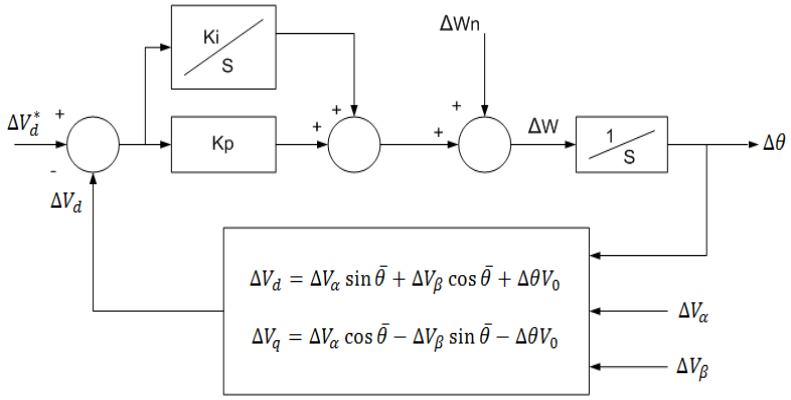

Fig.3.4: Small Signal Model of the PLL

Following the determination of an equivalent linear model, it is necessary to adopt some criteria in order to impose an adequate dynamic behavior on the three-phase PLL topology: By imposing an acceptable distance between the fastest pole and the sampling frequency of the DSP, one can guarantee the affective application of the PLL tracking commands. A better robustness of the three-phase PLL is achieved by imposing an adequate distance between closed-loop poles. The behavior of the PLL under distorted utility conditions is determined from the analysis of the dynamic stiffness of this topology. The closed-loop disturbance rejection characteristic of the three-phase PLL depends on the intended application. In systems where the fundamental component of the utility voltage vector must be tracked, it is necessary to elevate the dynamic stiffness figures in order to better reject undesired harmonic components. On the other hand, there are systems where the distortions present in the utility voltages might be known (e.g. for compensation actions) and thus the dynamic stiffness characteristics has to be shaped accordingly.

3.3.2 Synchronous Reference Frame (SRF)

Operation of a three phase SRF based PLL can be schematically shown in the Figure 3.5.

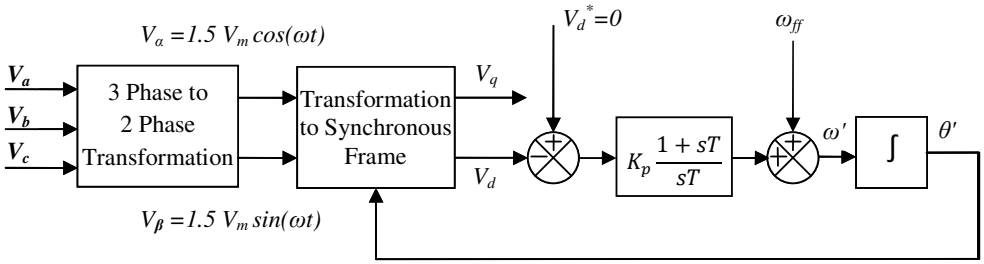

Fig.3.5: Schematic Diagram of SRF Based PLL

Basic structure of SRF PLL three phase voltage signals (Va, Vb and Vc) are transferred into stationary two phase system. Where,

$$V_a = V_m \cos(\omega t)$$

$$V_b = V_m \cos(\omega t - \frac{2\pi}{3})$$

$$V_c = V_m \cos(\omega t - \frac{4\pi}{3}) \qquad (3.18)$$

Now phase angle (θ) can be obtained by either synchronizing the voltage space vector (**V**, Fig.3.6) along q axis or along d-axis of synchronously rotating reference frame. Let us assume that the voltage space vector is to be aligned with q axis (Fig. 3.6).

$$\theta = \omega t - \frac{4\pi}{3}$$

Then position of d axis (θ) is related to it by integrating estimated frequency (ω′) which is the summation of output of PI controller and the feed-forward frequency (ωff). The voltage vectors in synchronously rotating reference frame can be found out using θ′ from following equations.

$$V_d = -\frac{3}{2} V_m \sin(\theta - \theta')$$

$$V_q = \frac{3}{2} V_m \cos(\theta - \theta')$$

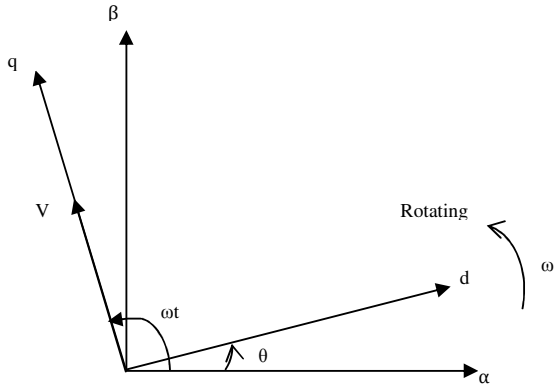

Fig.3.6. Vector Diagram Showing the Stationary ($\alpha\beta$) and Rotating (Dq) Reference Frames

The controller gains are designed such that Vd follows reference value which will result in estimated frequency (ω′) to lock to system frequency (ω) and estimated phase angle (θ′) to be equal to the phase angle θ. Now if θ = θ′ then space vector of voltage gets aligned to q axis. The voltage vector along synchronously rotating d-axis can be expressed as follows.

$$V_d = -\frac{3}{2}V_m(\theta - \theta')$$

So, overall system in Fig.3.5 can be simplified to that shown in Fig.3.7. Detailed analysis and design of PI controller gains can be found.

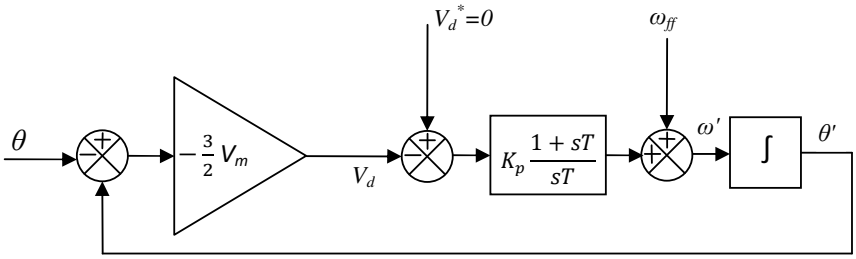

Fig.3.7 Block Diagram of SRF Based PLL Model

3.3.3 Double Synchronous Reference Frame (DSRF)

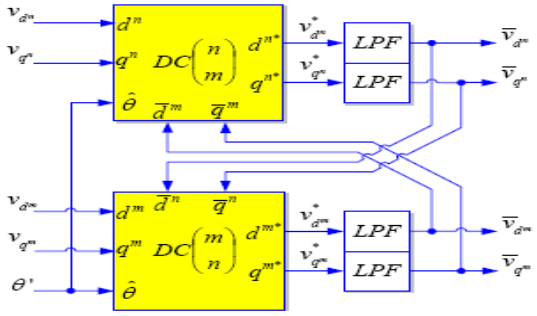

Fig.3.8: Decoupling Cell to Cancel the Effect of $\boldsymbol{V-1}$ on the $\boldsymbol{dq+1}$ Frame Signals

A voltage vector consisting of two generic components rotating with +ω and -ω frequencies respectively can be expressed on the αβ stationary reference frame as: [88]

$$V_{(\alpha\beta)} = \begin{bmatrix} V_\alpha \\ V_\beta \end{bmatrix} = V^{+1}_{(\alpha\beta)} + V^{-1}_{(\alpha\beta)} \\ = V^{+1}\begin{bmatrix} \cos(\omega t + \varphi) \\ \sin(\omega t + \varphi) \end{bmatrix} + V^{-1}\begin{bmatrix} \cos(-\omega t + \varphi) \\ \sin(-\omega t + \varphi) \end{bmatrix} \tag{3.19}$$

ω is the fundamental utility frequency.

Voltage vector of (3.19) will be expressed on the generic DSRF shown in Figure 3.8. This generic DSRF is composed of two rotating reference axes, $dq{+}1$ and $dq{-}1$, who"s angular positions are +θ and -θ respectively, being θ the phase angle detected by a hypothetical PLL. If a perfect synchronization of the hypothetical PLL was possible, that is if θ = ω*t* with ω the utility fundamental frequency, the voltage vector in (3.19) could be expressed on the $dq{+}1$ and $dq{-}1$ reference frames as (3.20) shows.

$$V_{(dq^{+1})} = \begin{bmatrix} V_{d^{+1}} \\ V_{q^{+1}} \end{bmatrix} = \left[T_{dq^{+1}}\right] V_{(\alpha\beta)} \\ = V^{+1}\begin{bmatrix} \cos\varphi \\ \sin\varphi \end{bmatrix} + V^{-1}\cos\varphi^{-1}\begin{bmatrix} \cos 2\omega t \\ -\sin 2\omega t \end{bmatrix} + V^{+1}\sin\varphi^{+1}\begin{bmatrix} \sin 2\omega t \\ \cos 2\omega t \end{bmatrix} \tag{3.20}$$

$$V_{(dq^{+1})} = \begin{bmatrix} V_{d^{+1}} \\ V_{q^{+1}} \end{bmatrix} = \left[T_{dq^{+1}}\right] V_{(\alpha\beta)} \\ = V^{-1}\begin{bmatrix} \cos\varphi^{-1} \\ \sin\varphi^{-1} \end{bmatrix} + V^{+1}\cos\varphi^{+1}\begin{bmatrix} \cos 2\omega t \\ \sin 2\omega t \end{bmatrix} + V^{+1}\sin\varphi^{+1}\begin{bmatrix} -\sin 2\omega t \\ \cos 2\omega t \end{bmatrix} \tag{3.21}$$

$$\left[T_{dq^k}\right] = \begin{bmatrix} \cos(k\theta) & \sin(k\theta) \\ -\sin(k\theta) & \cos(k\theta) \end{bmatrix}; k = +1, -1 \tag{3.22}$$

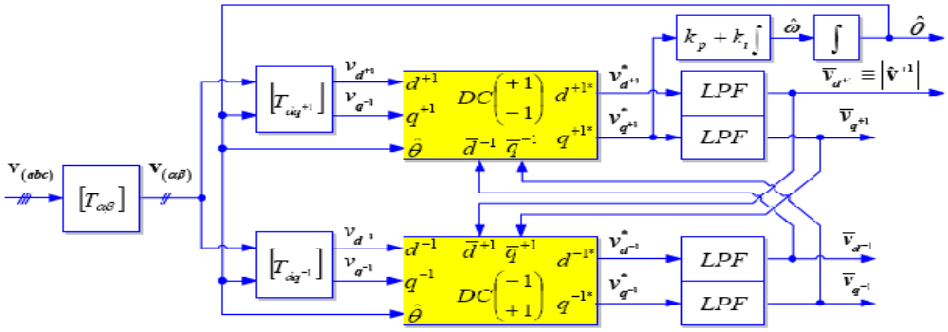

Fig.3.9: Block Diagram of DSRF PLL

In (3.20), the amplitude of the signal oscillation in the dq+1 axes depends on the mean value of the signal in the $dq-1$ axes, and vice versa. In order to cancel the oscillations in the dq+1 axes signals, the decoupling cell shown in Figure 3.8 is proposed. For cancelling oscillations out in the dq+1 axes signals, the same structure may be used but interchanging (-1) by (+1) in it.

In this work, the accurate detection of the parameters is achieved by means of the cross-feedback decoupling network (DN) shown in the model in Fig.3.9. In this DN the LPF block represents a first order low-pass filter with ωf (cut-off frequency). A detailed analysis of the DN was done and it was concluded that, after a stabilization period, the signal on the axes DSRF are free of oscillations and the amplitude of the (-1) and (+1) components are accurately determined. After the analysis of the DN, it seems reasonable to set the cut-off frequency of the low-pass filter ωf around $\omega/2$, ω being the estimated fundamental utility frequency. This value for the cut-off frequency achieves a fast enough dynamic response and avoids transient oscillations in the output signals of the DN.

3.4 Load Sharing Techniques:

Different load sharing techniques are available for parallel operation of DGs, they are

i. Droop method
ii. Master-Slave method

3.4.1 Droop method:

Theoretical Background:

The power flowing into a line at point A, as represented in Fig. 3.10,

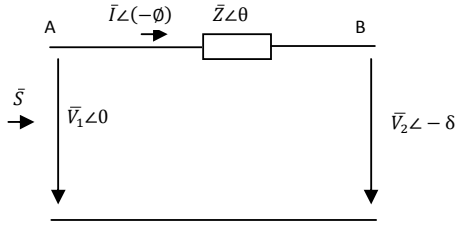

Fig.3.10: Power flow through a line

$$P + jQ = \bar{S} = \bar{V}_1\bar{I}^* = \bar{V}_1\left(\frac{\bar{V}_1 - \bar{V}_2}{\bar{Z}}\right)^*$$

$$= V_1\left(\frac{V_1 - V_2 e^{j\delta}}{Ze^{-j\theta}}\right)$$

$$= \frac{V^2{}_1}{Z}e^{j\theta} - \frac{V_1V_2}{Z}e^{j(\theta+\delta)} \qquad (3.23)$$

Thus, the active and reactive power flowing into the line is

$$P=\frac{V_1^2}{Z}\cos(\theta+\delta)-\frac{V_1V_2}{Z}\cos(\theta+\delta) \quad (3.24)$$

$$Q=\frac{V_1^2}{Z}\sin(\theta)-\frac{V_1V_2}{Z}\sin(\theta+\delta) \quad (3.25)$$

With $Ze^{j\theta}=R+jX$,(3.24) and (3.25) are written as

$$p=\frac{V_1}{R^2+X^2}[R(V_1-V_2\cos\delta)+XV_2\sin\delta] \quad (3.26)$$

$$Q=\frac{V_1}{R^2+X^2}[-RV_2\sin\delta+X(V_1-V_2\cos\delta)] \quad (3.27)$$

or

$$v_2\sin\delta=\frac{XP-RQ}{V_1} \quad (3.28)$$

$$V_1-V_2\cos\delta=\frac{RP+XQ}{V_1} \quad (3.29)$$

For overhead lines X >> R, which means that R may be neglected. If also the power angle is small, then $\sin\delta=\delta$ and $\cos\delta=1$. Equations (3.28) and (3.29) then become

$$\delta\cong\frac{XP}{V_1V_1} \quad (3.30)$$

$$V_1-V_2\cong\frac{XQ}{V_1} \quad (3.31)$$

For X>>R, a small power angle δ and voltage difference V_1-V_2, (3.30) and (3.31) show that the power angle depends predominantly on P, whereas the voltage difference depends predominantly on Q. In other words, the angle can be controlled by regulating P, whereas the inverter voltage V_1 is controllable through Q. Control of the frequency dynamically controls the power angle and, thus, the real power flow. Thus, by adjusting P and Q independently, frequency and amplitude of the grid voltage are determined. These conclusions form the basis for the well-known frequency and voltage droop regulation through respectively active and reactive power

$$f-f_o=-k_p(P-P_o) \quad (3.32)$$

$$V_1-V_o=-k_q(Q-Q_o) \quad (3.33)$$

f_o and V_o are rated frequency and grid voltage respectively, and P_o and Q_o are the (momentary) set points for active and reactive power of the inverter. The frequency and voltage droop control characteristics are shown graphically in Fig. 3.11.

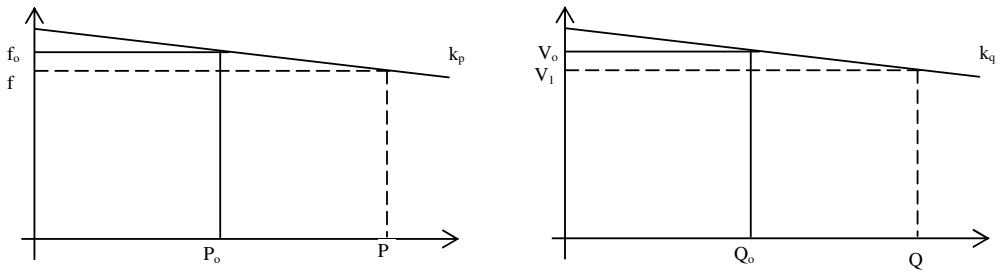

Fig.3.11: frequency and voltage droop control characteristics.

For distributed grid R is no longer neglected since their line is considered mainly resistive. Therefore in the present case, X could be neglected instead of R. In this case, adjusting active power influences the voltage amplitude, while, adjusting reactive power influences the frequency. Relationships have changes radically, in such a way that the droop regulation described by (3.32) and (3.33) is no longer effective.

As a general case, both X and R is to be considered. Then, the use of an orthogonal linear rotational transformation matrix 'T' from active and reactive power 'P' and 'Q' to the "modified" active and reactive power 'P'' and 'Q'' is proposed

$$\begin{bmatrix} P' \\ Q' \end{bmatrix} = T \begin{bmatrix} P \\ Q \end{bmatrix} = \begin{bmatrix} \sin\theta & -\cos\theta \\ \cos\theta & \sin\theta \end{bmatrix} \begin{bmatrix} P \\ Q \end{bmatrix} = \begin{bmatrix} \frac{X}{Z} & -\frac{R}{Z} \\ \frac{R}{Z} & \frac{X}{Z} \end{bmatrix} \begin{bmatrix} P \\ Q \end{bmatrix} \qquad (3.34)$$

Applying this transformation on (4) and (5) results in

$$\sin\delta = \frac{ZP'}{V_1 V_2} \qquad (3.35)$$

$$V_1 - V_2\cos\delta = \frac{ZQ'}{V_1} \qquad (3.36)$$

For a small power angle δ and voltage difference V_1-V_2, (3.35) and (3.36) show that the power angle depends only on P', whereas the voltage difference depends only on Q'. In other words, the angle can be controlled by regulating P', whereas the inverter voltage V_1 is controllable through Q'. As the grid frequency is influenced through the angle δ, the definition of P' and Q' permits independent influence the grid frequency and amplitude. Fig. 3.12 depicts effect of P', Q', P, and Q on voltage and frequency by considering different ratios of R/X. To derive P' and Q', it suffices to know the X/R ratio and knowledge of the absolute values of the line impedance is not needed$\left(\emptyset = \pi - \theta = a\tan\left(\frac{R}{X}\right)\right)$.

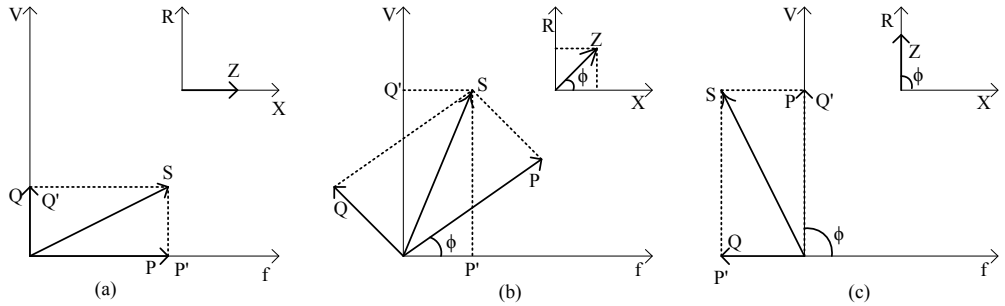

Fig 3.12: Influence of active and reactive power on voltage and frequency for different line impedance ratio: (a) R/X = 0, (b) R/X = 1, (c) R/X = ∞.

From Fig. 3.12, it is clear that for mainly inductive lines P'≈P and Q'≈Q, whereas for mainly resistive lines P'≈–Q and Q'≈P. Hence, the frequency and voltage droop regulation becomes

$$f - f_o = -k_p(P' - P_o') = -k_p\frac{X}{Z}(P - P_o) + k_p\frac{R}{Z}(Q - Q_o) \quad (3.37)$$

$$V_1 - V_2 = -k_q\left(Q' - Q_0'\right) = k_q\frac{R}{Z}(P - P_0) - k_q\frac{X}{Z}(Q - Q_0) \quad (3.38)$$

3.4.2 Master-Slave:

In Master Slave technique one DG unit acts as “Master” and sets the voltage and frequency of the microgrid in islanded mode, while other units adops the voltage and frequency from Master, and in grid connected mode all DGs operate in current control mode as shown in Fig.2.5.The DG unit with highest rating is often favourable to act as “Master”. The DGs can control in two ways

i. With centralized control
ii. With decentralized control

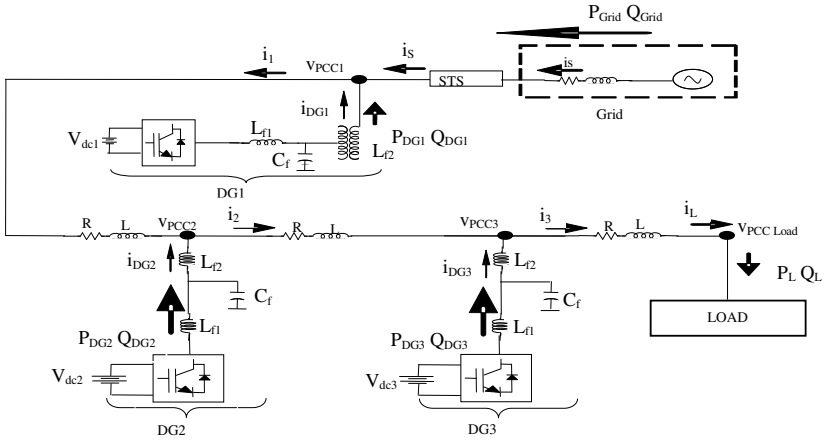

Fig 3.13: Microgrid in grid connected mode

System Configuration:

Fig.3.13 depicts the schematic diagram of considered microgrid which is connected to mains through a static transfer switch (STS). The considered micro grid comprises of three DG's (DG1, DG2 and DG3), and local RL load, connected in parallel through a single distributed line. The considered DG's are comprised of micro sources with battery support and are represented by a battery. The LCL filter at the terminals of each VSC reduces the harmonics in the line. At every node current sensing is done in micro grid for exact computation of the loads. In case the load is connected to one end and sources to the other, this configuration eases out the use of extra sensors for load estimation to generate the references, which in turn decreases the cost and complexity of the microgrid formation. The system is in 'Master-Slave' configuration operating in current controlled mode, with the supply grid acting as the master in grid connected mode, and, DG-1 acting as master in islanded/standalone mode. The DG sources are invariably configured to work as current source adding current to the nodes. Any perturbation in load power is catered by DG sources, upto their capability. In the Islanded/standalone mode the voltage template of the erstwhile grid tied mode is freezed by the PLL which provides the reference template to the Master DG for generation of voltage by switching the mode from current control mode to PWM mode.

i. With centralized control:

Control Scheme:

Fig.3.14 depicts the block diagram of control scheme of Master Slave with communication for centralized control adopted for the proposed microgrid. The control scheme is based on demand and supply equilibrium.

The sensed load current demand was transformed from abc to dq frame by using park's transformation (3.39), the sine and cosine signals for transformation is obtained from load PCC point.

$$\begin{bmatrix} f_d \\ f_q \end{bmatrix} = M(\theta) \begin{bmatrix} f_a \\ f_b \\ f_c \end{bmatrix}, \tag{3.39}$$

$$M(\theta) = R(\theta)C = \frac{2}{3} \begin{bmatrix} \cos(\theta) & \cos\left(\theta - \frac{2\pi}{3}\right) & \cos\left(\theta - \frac{4\pi}{3}\right) \\ \sin(\theta) & \sin\left(\theta - \frac{2\pi}{3}\right) & \sin\left(\theta - \frac{4\pi}{3}\right) \end{bmatrix},$$

Where

$$R(\theta) = \begin{bmatrix} \cos\theta & \sin\theta \\ -\sin\theta & \cos\theta \end{bmatrix}$$

Where $\theta = \omega t$ and ω is the frequency of the electric system, and

$$C = \begin{bmatrix} 1 & -\frac{1}{2} & -\frac{1}{2} \\ 0 & \frac{\sqrt{3}}{2} & -\frac{\sqrt{3}}{2} \end{bmatrix}.$$

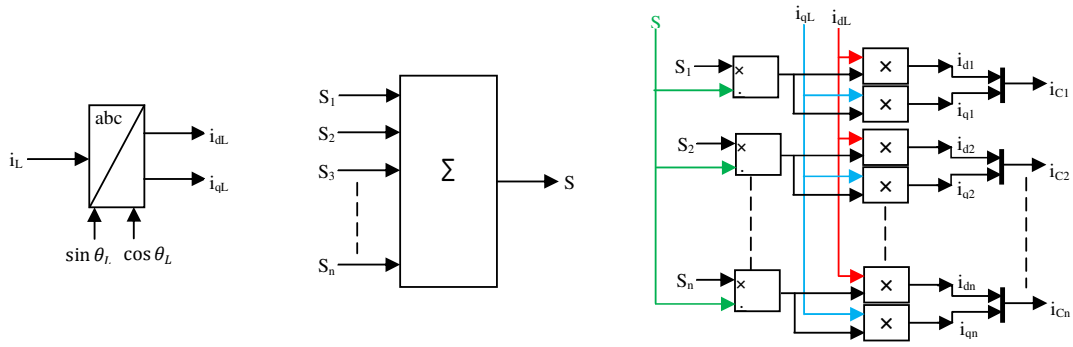

Fig. a: Centralized Control Unit

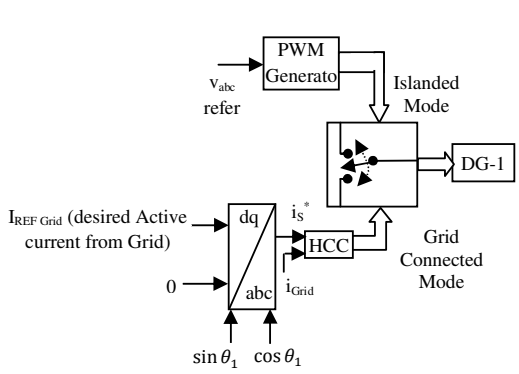

Fig.b: Control scheme for Master

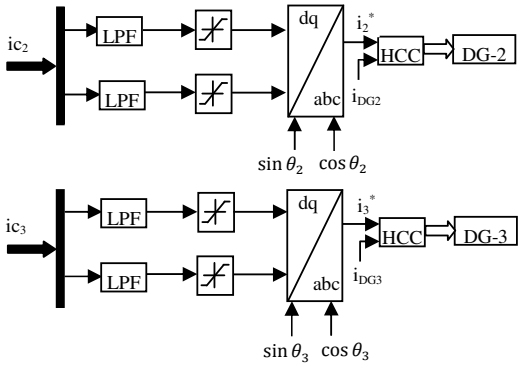

Fig.c: Control Slave

Fig. 3.14: Control Scheme for Master and Slaves in centralized control

The centralised control unit shown in Fig.3.14-a generates the current commands in dq frame for all DG's for real and reactive power according to their ratings.

S1, S2, S3, S4, --------Sn are the rating of DG_1, DG_2, DG_3, DG_4, ---------- DG_n. and W_1, W_2, W_3, W_4, --------W_n are the weights of DGs. Whenever DG is active then its weight is one other wise zero.

Total rated capacity of Micro Grid is given by

$$S = W_1S_1 + W_2S_2 + W_3S_3 + W_4S_4 + \text{--------} + W_nS_n \qquad (3.40)$$

Reference current signal for K^{th} DG_k is given by

$$i_{CK} = i_L \times \frac{W_K S_K}{S} \text{ (where k=1,2,3,-------,n)} \qquad (3.41)$$

Where S_K is the rating of K^{th} DG and i_L is the total load current.

Fig.3.14-b and Fig.3.14-c depicts the basic control block for master and slaves respectively. It comprises of a low pass filter, saturation block, dq/abc conversion, PWM generator and hysteresis current controller (HCC) for control of the VSC's such that commanded reference current is tightly followed. Fig.3.14-c depicts the command reference obtained from central

controller in dq frame for slave DGs which is filtered by LPF are then reverse park transformed to three phase reference AC currents. The reference currents so obtained when compared with actual currents of the DG, in the HCC, it provides gating signals for the corresponding VSCs.

Fig.3.14-b shows the control scheme of DG1. When the microgrid is operating in grid connected mode The DG1 is operated in indirect current control mode in order to keep mains as constant source at unity power factor. Whenever the reference voltage and frequency for all DGs in the microgrid, which are getting from mains are not in standard then the microgrid is islanded from the mains. In Islanded mode, DG1 is operated in voltage control mode to maintain the micro grid voltage and frequency, to facilitate the operation of other slave DG's to continue operating in current control mode the control for other DGs acts similar to DG's when the microgrid is operating in grid connected mode, where as in islanded mode.

ii. With decentralized control:

Fig.3.15 depicts the block diagram of control scheme of Master Slave without communication (decentralized control) adopted for the proposed microgrid. It comprises of a low pass filter, gain, saturation block, abc/dq and dq/abc conversions, PWM generator and hysteresis current controller (HCC) for control of the VSC's such that commanded reference current is tightly followed. In this method the sharing has been done with the help of the local measurement and the capacities of DGs.

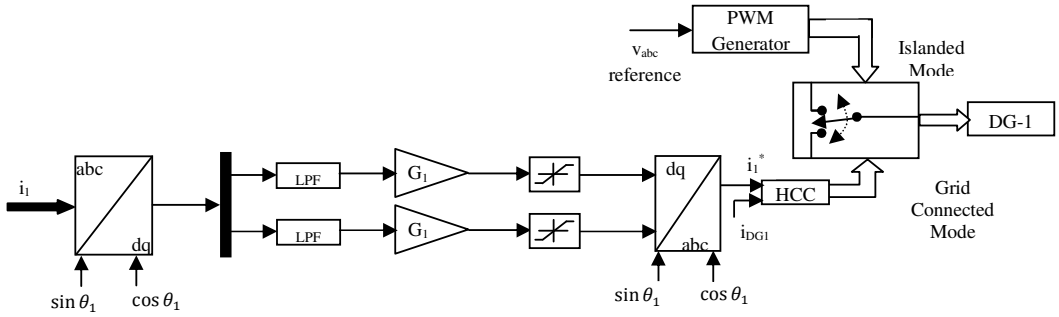

a: Control scheme for Master DG

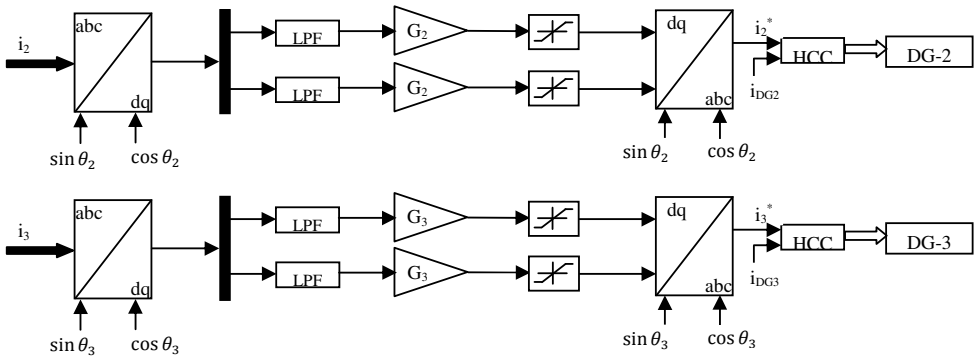

b: Control Scheme for slave DGs

Fig.3.15: Control Scheme for Master and Slaves in decentralized control

The capacities of DGs represented as gains are given by

$$G_1 = \frac{S_1}{S-(S_2+S_3+----+S_n)}$$,where G_1 is the capacity gain of DG1

$$G_2 = \frac{S_2}{S-(S_3+4+-----+S_n)}$$, where G_2 is the capacity gain of DG2

So on $$G_k = \frac{S_k}{S-(S_{K+1}+S_{K+2}+----+S_n)}$$, where G_k is the capacity gain of DGn

and so on $$G_n = \frac{S_n}{S}.$$ (3.42)

where G_n is the capacity gain of DGn.

Fig 3.15-a shows the control scheme of DG1. When the microgrid is operating in grid connected mode the DG1 control scheme is same as other slave DGs. Whenever the reference voltage and frequency for all DGs in the microgrid, which are getting from mains are not in standard then the microgrid is islanded from the mains. In Islanded mode, DG1 is operated in voltage control mode to maintain the micro grid voltage and frequency, to facilitate the operation of other slave DG's to continue operating in current control mode. The control automatically shares the load between the slaves and DG1. The DG1 is relatively lesser loaded as compared to its capacity, since the load is little skewed distributed. Further to enhance the reliability of the operation of microgrid the capacity of DG1 may be reduced in calculation of reference to create a room for transient handling by rescuing the capacity in actual during operation. For present case capacity of master in islanded mode is assumed 50% of actual for estimation of command references for each DG.

Fig.3.15-b depicts the current control operation of DG2 and DG3. The current which is sensed at the respective PCC point of DG is transformed from abc to dq frame by using park's transformation (3.39). The sine and cosine synchronizing signals are derived at each node by separate PLL at each PCC.

Obtained dq currents are filtered through LPF and multiplied with respective gains, then inverse park transformed to get three phase reference AC currents. The reference currents for each DG so obtained when compared with actual currents of each DG, in the respective HCC, it provides gating signals for the corresponding VSCs.

CHAPTER-4

MATLAB SIMULATION MODLE AND PERFOMANCE EVALUATION

4.1 GENERAL

The performance of the system is evaluated using the MATLAB Simulink for current controlled in master slave configuration both in grid connected and islanded modes. The master DG is considered operating in voltage control mode under islanded mode. The results are discussed for load sharing, transient operation for load and DGs in microgrid for both grid connected and islanded mode of operation.

4.2 Performance evaluation of proposed microgrid with centralized current control of DGs:

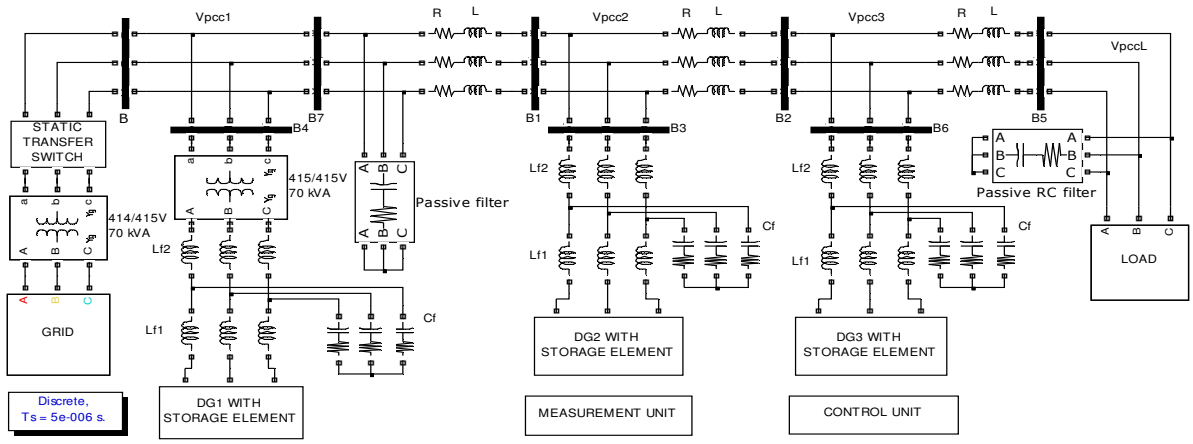

Fig.4.1: Simulink model of the considered microgrid with centralized current control of DGs

The Grid, Isolation transformer, DGs with input side LCL filter, STS, Control unit, distributed line impedance respected as RL line impedance, three phase RL load and passive RC filter are modelled in MATLAB using Power System Block set. Fig.4.1 depicts the setup used to study the performance of the Microgrid in Grid connected mode/Islanded mode with proposed control scheme through simulation.

The Grid block consists of a three-phase voltage source acting as “infinite bus” supplying the microgrid to gauge the performance of the Microgrid with proposed scheme under specified conditions is assumed. The considered loads to evaluate the effectiveness of the proposed scheme are star connected 100 KVA RL load at 0.8 pf depicted in Fig.4.1. Out of this load 35 KVA load is considered critical, which is required to be supported all the times. The RC high pass passive filter is used to absorb the harmonics in voltage at load terminals. The Intentional islanding has been done with the help STS to study the

performance of micro grid in Islanded mode. The simulated results are studied to gauge the performance of Microgrid under both grid connected/Islanded modes. Table 4.1 depicts parameters of the considered system.

TABLE 4.1. PARAMETERS OF THE CONSIDERED SYSTEM FOR CENTRALIZED CURRENT CONTROL OF DGS

DG1 Power Rating	40 KVA
DG2 Power Rating	25 KVA
DG3 Power Rating	15 KVA
Isolated Transformers Power rating	100 KVA
Line Impedance	0.01334 Ω, 0.03 mH
Load	35-100 KVA at 0.8 pf
LCL filter (L_{f1}, C_f, L_{f2})	1.5 mH, 15 μF, 0.5 mH
Passive filter (RC)	1Ω, 100μF
Passive filter	1μF
DC Voltage (Each DG)	800v

The performance of the system is studied under two cases normally: Grid connected mode and Intentional Islanding mode.

4.2.1. Grid connected mode:

The mains is considered supplying constant power of 26.7 KW to the microgrid, and the balance power is supplied by the active DG's in the microgrid. It may be observed from Fig.4.3, that initial load demand of 72.67 KVA at 0.8 pf is catered by mains which contributes 27.5KW, and the remaining 34 KW and 40 KVAR demand is contributed by DG's depending upon their ratings as 19.7 KW and 21.98 KVAR, 10.54 KW and 12.8 KVAR and 5.91 KW and 7.63 KVAR respectively from DG1, DG2 and DG3 (including microgrid losses). It may also observe that current drawl from the mains is at unity power factor where current is shown to be in phase with the voltage. From Fig.5 it may be observed that, the transients due to disturbances like load perturbations, DG failures ect. is taken care by the DG1. Starting at t=0, during the transient period the active and reactive power contribution by DG1 is increased from 0 KW to 24.1 KW and 0 KVAR to 26 KVAR, and after the transient period the active and reactive power contribution of DG1 is settled to 19.7 KW and 21.98 KVAR. When at t=0.1s the load is increased to 95.87 KVA at 0.825 pf, the increased demand is supplied by the active DG's in the system depending upon their ratings as 29.2 KW and 29.61 KVAR, 16.55 KW and 17.37 KVAR and 9.5 KW and 10.31 KVAR respectively from DG1, DG2 and DG3 where as the main's contribution remains constant. During transient period the active and reactive power contribution of DG1 is increased from 19.7 KW to 31.5 KW and 21.98 KVAR to 31 KVAR, and after the transient period the active and reactive power contribution by DG1

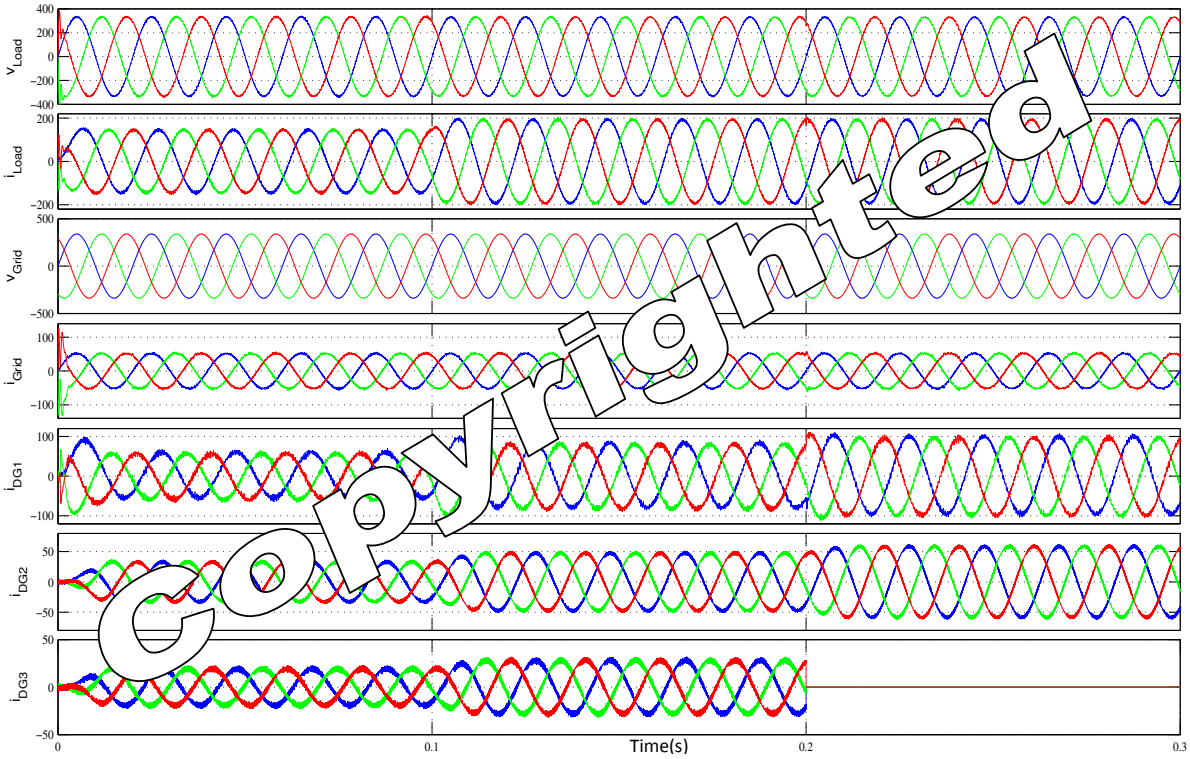

Fig.4.2: Current and Voltage wave forms of Microgrid under Grid connected mode in centralized current control of DGs

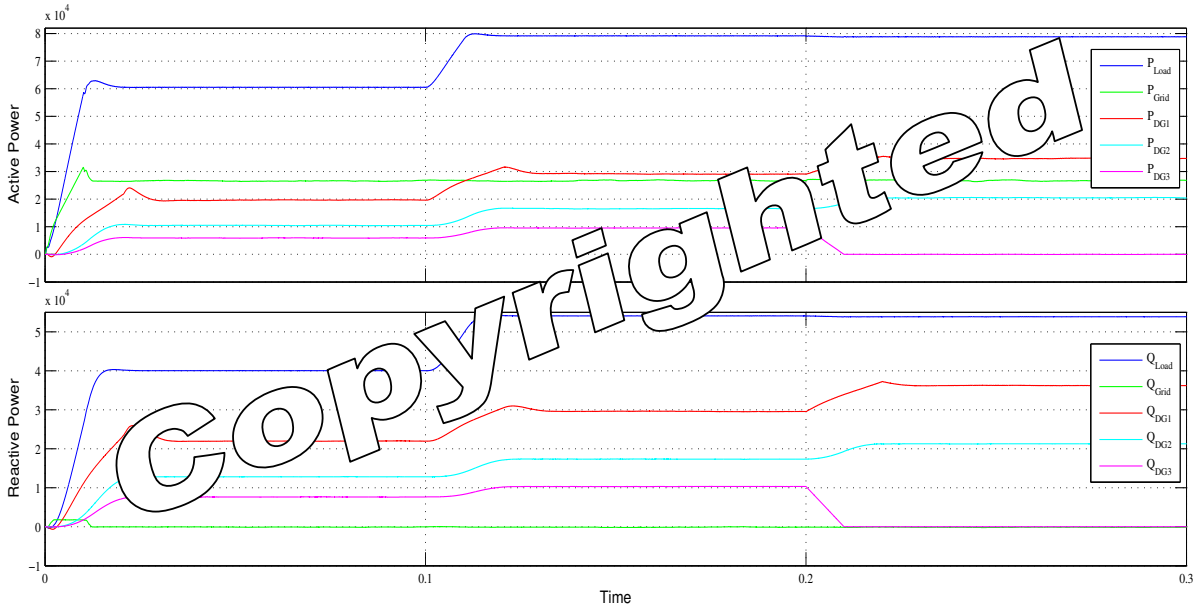

Fig.4.3: Active and Reactive Power wave forms of Microgrid under Grid connected mode in centralized current control of DGs

is settled to 29.2 KW and 29.61 KVAR. At t=0.2 sec, DG3 fails, ultimately making the current IDG-3 =0, its share of power is then contributed by other DG's which are active according their ratings as 34.7 KW and 36.2 KVAR and 20.6 KW and 21.25 KVAR respectively from DG1 and DG2.

4.2.2. Islanded mode:

Control of DGs become critical while its operation in islanded mode amidst their limited capacities. It is therefore load corresponding to sum of capacities of slave DGs and 50%

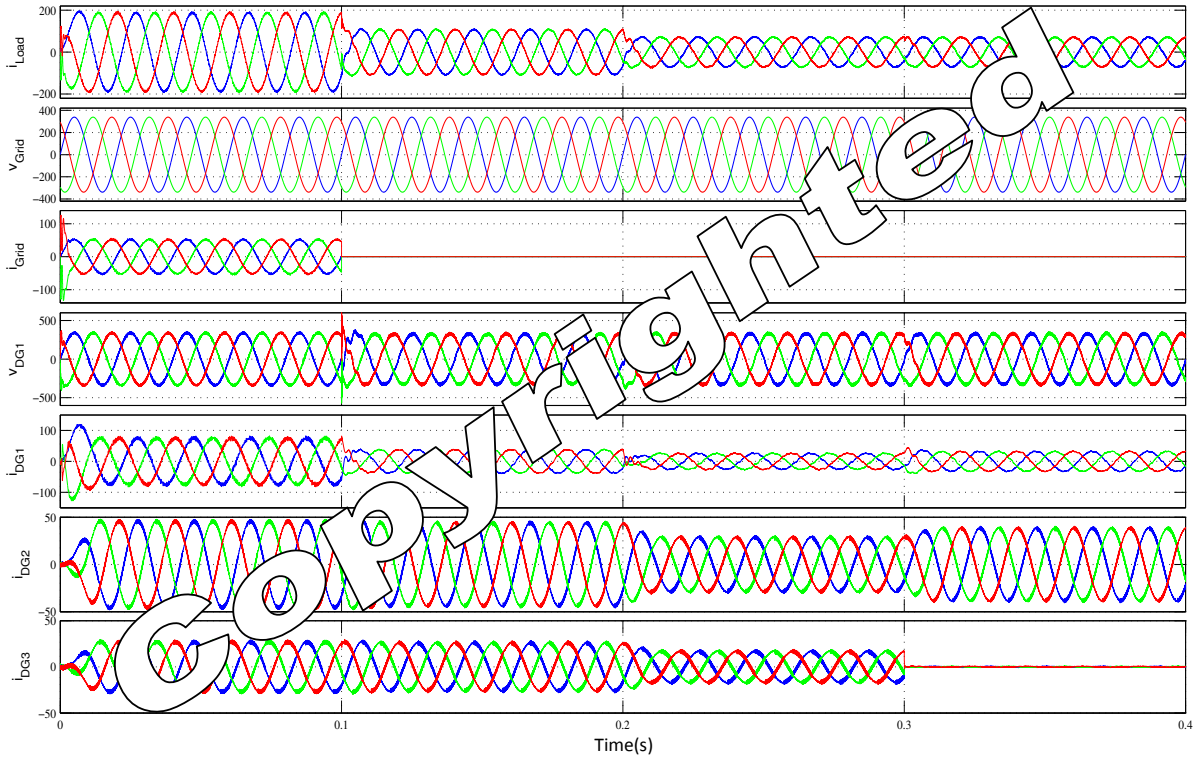

Fig.4.4: Current and Voltage wave forms of Microgrid under Islanded mode in centralized current control of DGs

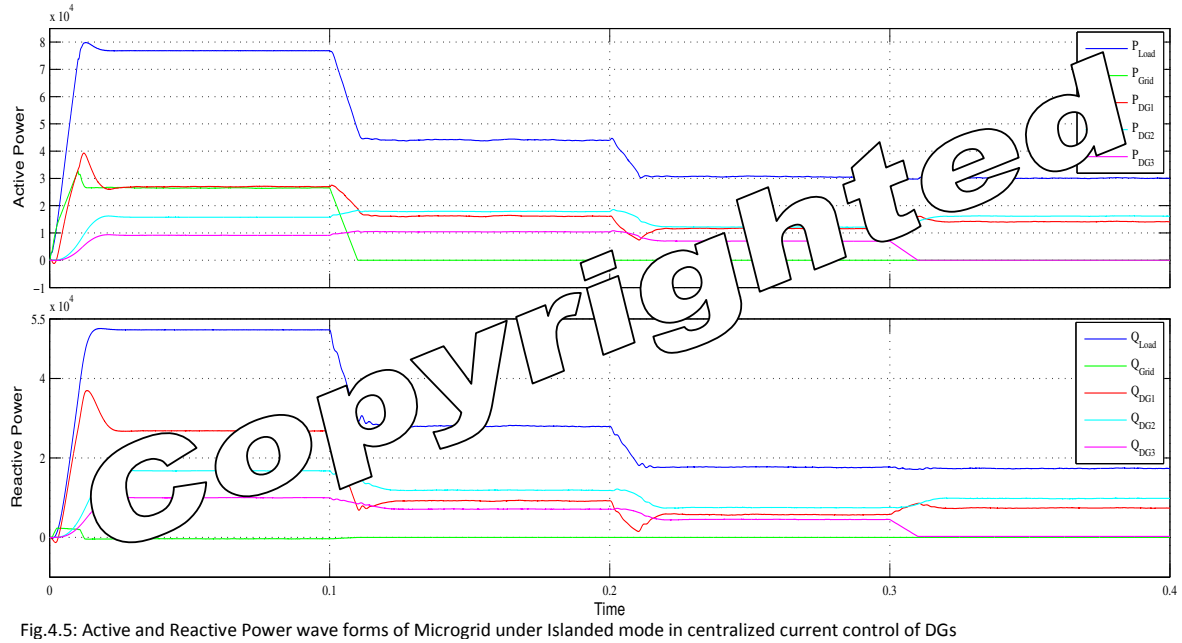

Fig.4.5: Active and Reactive Power wave forms of Microgrid under Islanded mode in centralized current control of DGs

capacity of master DG is kept in the Islanded microgrid and remaining non critical load is shedded. The shedding of the non-critical load is done in a chunk as soon as islanded condition is detected. Fig.4.4 depicts the microgrid response to load perturbations and failure of DG3 from the microgrid. From t=0s to t=0.1s the grid connected operation is considered, accordingly connected load of 93 KVA at 0.82 pf is supported. The contribution of mains remains of 26.7 KW and remaining power of 50.15 KW and 52.22 KVAR is shared by DG's as per their ratings as 27 KW and 26.82 KVAR, 15.7 KW and 12.8 KVAR and 5.91 KW and 7.63 KVAR respectively from DG1, DG2 and DG3 (including microgrid losses). At t=0.1s it may be observed that microgrid is islanded from mains and connected load is reduced to 52 KVA at 0.84 pf. It may further be observed that distortion due to switching is now present due to DG1 taking over as a voltage source. It may also be clear that transition of DG1 from current source to voltage source is made with in half cycle and voltage is restored almost instantly with freezed synchronizing template such that operation of DGs are not distributed, and they share the load as per their rating as 18.45 KVA at 0.86 pf, 21.3 KVA at 0.83 pf and 12.6 KVA at 0.82 pf from DG1, DG2 and DG3 respectively, maintaining sinusoidal current wave shape (refer Fig.4.4). At t=0.2s load is decreased to 35 KVA at 0.85. pf to match the local generation by DGs. The power is accordingly shared as 13 KVA at 0.9 pf, 14 KVA at 0.85 pf and 8.32 KW at 0.85 pf between DG1, DG2 and DG3. As explained before in grid connected mode, here also the transient was taken care by DG1, its contribution is decreased from 16 KW to 7.419 KW and 9.2 KVAR to 1.5 KVAR. After the transient period its contribution is settled to11.6 KW and 5.7 KVAR. It may be observed that the capacity of DG1 is not breached even if it is acting as a voltage source. When at t=0.3s DG3 fails, its capacity is shared between DG1 and DG2 as 15.9 KVA at 0.88 pf and 18.84 KVA at 0.85 pf respectively by ensuring that capacity of DG1 is never breached. In Fig.4.5 it may be observed that DG2 has shared the load greater than the corresponding ratio.

4.3 Performance evaluation of proposed microgrid with decentralized current control of DGs:

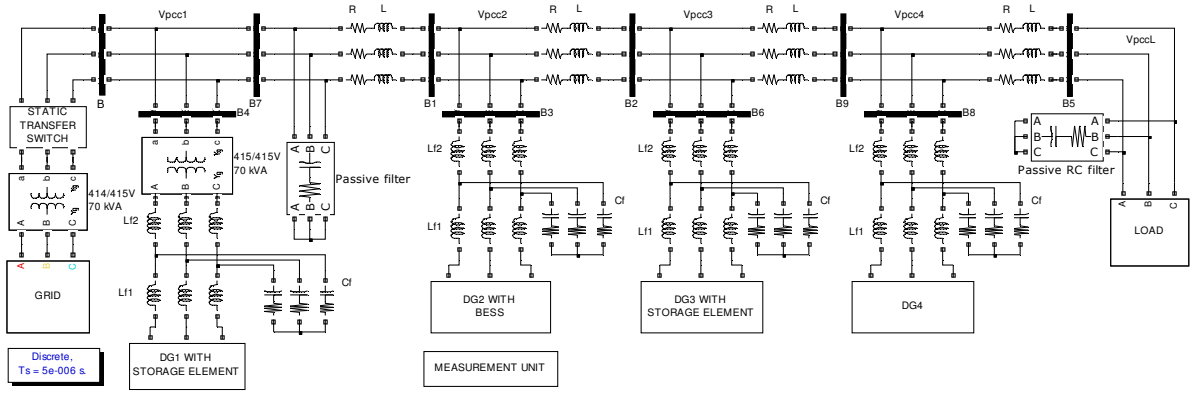

Fig.4.6: Simulink model of the considered microgrid with decentralized current control of DGs

The simulated results are studied to gauge the performance of Microgrid under grid connected/Islanded modes. Table I depicts parameters of the considered system.

TABLE 4.2. PARAMETERS OF THE CONSIDERED SYSTEM FOR DECENTRALISED CURRENT CONTROL OF DGS

DG1 Power Rating	50 KVA
DG2 Power Rating	30 KVA
DG3 Power Rating	20 KVA
Isolated Transformers Power rating	100 KVA
Line Impedance	0.01334 Ω, 0.03 mH
Load	15-100 KVA at 0.8 pf
LCL filter (L_{f1}, C_f, L_{f2})	1.5 mH, 15 µF, 0.5 mH
Passive filter (RC)	1Ω, 100µF
Passive filter	1µF
DC Voltage (Each DG)	800v

4.3.1. Grid connected mode:

It may be observed from Fig 4.7, that initial load demand of 60.7 KW and 40.15KVAR is shared by DG's depending upon their ratings which are respectively as 31.3 KW and 20.8 KVAR, 18.75 KW and 12.75 KVAR and 10.7 KW and 7.62 KVAR from DG1, DG2 and DG3 (including microgrid losses). Very small power is contributed by mains 2 KW and 1.1 KVAR to justify its physical existence. From Fig 4.8 it may be observed that, the transients due to disturbances like load perturbations, DG failures etc. is taken care by the mains. After starting at t=0, the active and reactive power contribution of mains is settled to 2 KW and 1.1 KVAR. Whereas during the transient period the active and reactive power peak takes 12.8 KW and 7.6 KVAR. At t=0.1s, where the load is increased to 79.4 KW and 54.25 KVAR, the increased demand is supplied by the active DG's in the system depending upon their ratings as 40.85 KW and 28.5 KVAR, 24.85 KW and 17.3 KVAR and 14.25 KW and 10.3 KVAR

respectively from DG1, DG2 and DG3. During transient period the active and reactive power peak takes 5.61 KW and 3.5 KVAR from mains, and after the transient period the active and reactive power contribution by mains is settled back to 2 KW and 1.1 KVAR. At t=0.2 sec, DG3 fails, ultimately its share of power is then contributed by other DG's which are active, accordingly their rating are as 49.6 KW and 35.2 KVAR and 30.3 KW and 21.2 KVAR respectively from DG1 and DG2. The transient here also is contributed by mains, During transient period the active and reactive power peak takes 4.8 KW and 3 KVAR, and after the transient period the active and reactive power contribution by mains is settled back to 2 KW

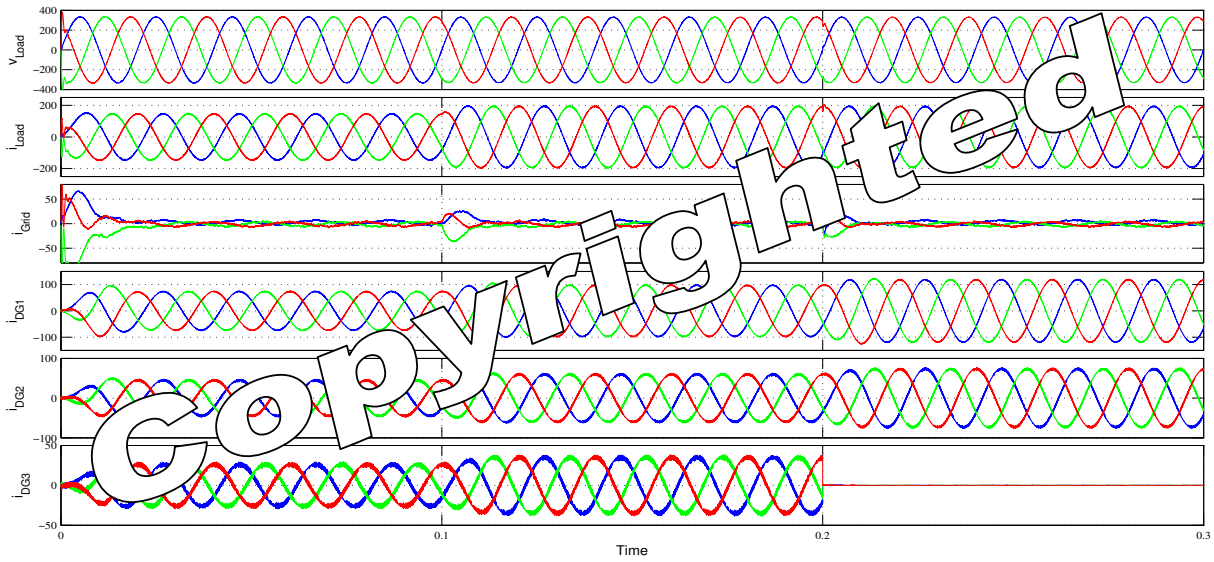

Fig 2.7: Current and Voltage wave forms of Microgrid under Grid connected mode in decentralized current control of DGs

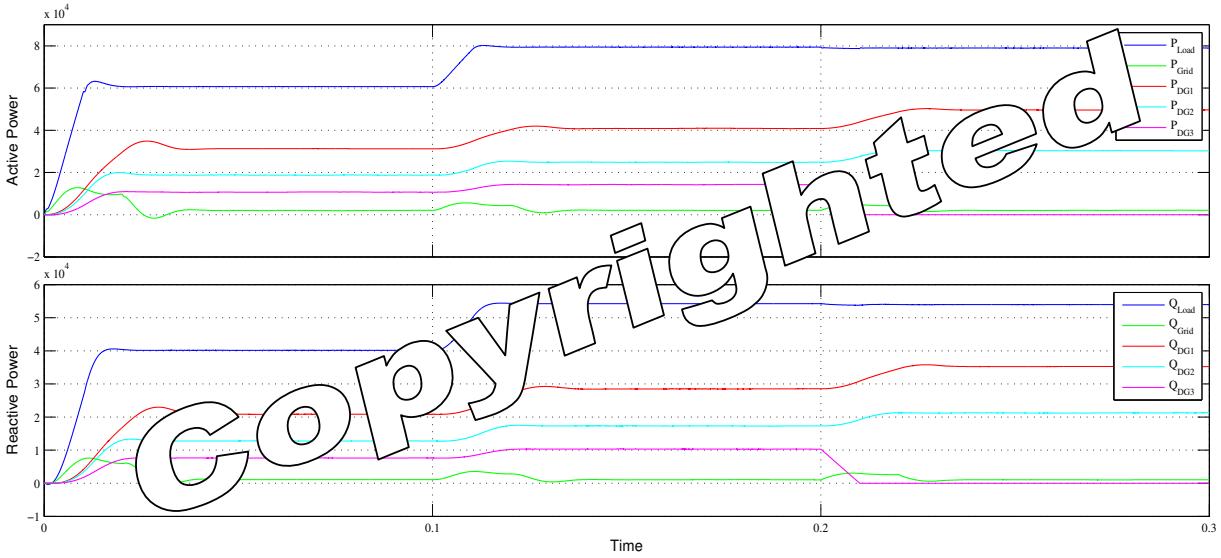

Fig 4.8: Active and Reactive Power wave forms of Microgrid under Grid connected mode in decentralized current control of DGs

and 1.1 KVAR.

4.3.2. Islanded mode :

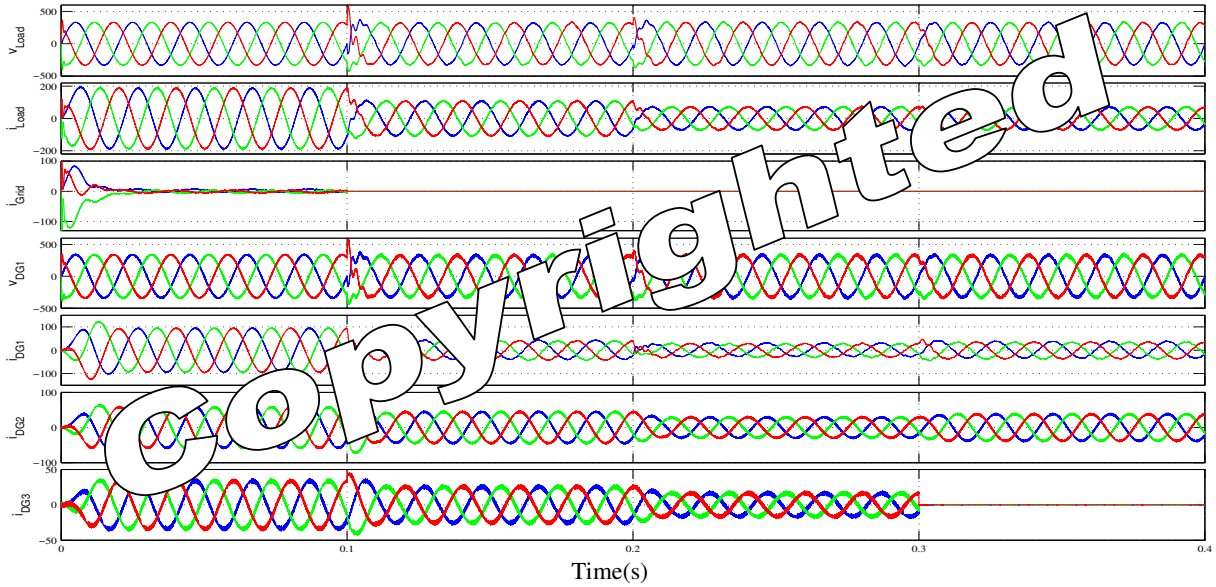

Fig 4.9: Current and Voltage wave forms of Microgrid under Islanded mode in decentralized current control of DGs

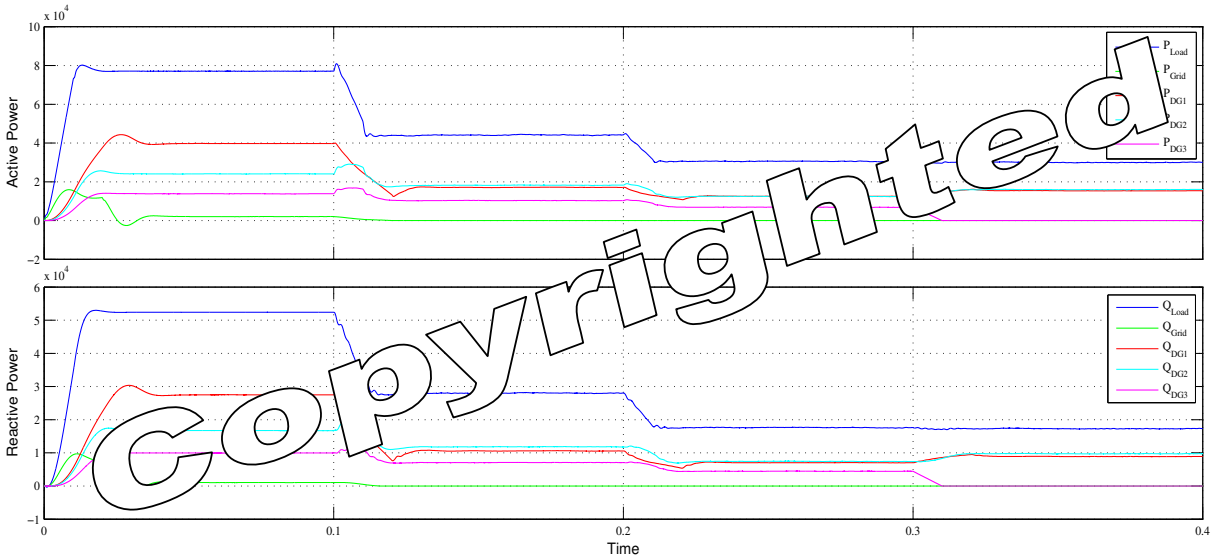

Fig 4.10: Active and Reactive Power wave forms of Microgrid under Islanded mode in decentralized current control of DGs

Control of DGs become critical while its operation in islanded mode amidst their limited capacities is performed. It is therefore load corresponding to sum of capacities of slave DGs and 50% capacity of master DG is kept in the Islanded microgrid and remaining non critical load is shedded. The shedding of the non-critical load is done in a chunk as soon as islanded condition is detected. Fig.4.9 depicts the microgrid response to load perturbations and failure of DG3 from the microgrid. From t=0s to t=0.1s the grid connected operation is

considered, accordingly connected load of 77.05 KW and 52.4 KVA is supported. The power is shared by DG's as per their ratings as 27 KW and 26.82 KVAR, 15.7 KW and 12.8 KVAR and 5.91 KW and 7.63 KVAR respectively from DG1, DG2 and DG3 (including microgrid losses). A very small power from mains of 2 KW and 1 KVAR is drawn. At t=0.1s it may be observed that microgrid is islanded from mains and connected load is reduced to 44 KW and 27.9 KVAR. It may further be observed that distortion due to switching is now present due to DG1 taking over as a voltage source. It may also be clear that transition of DG1 from current source to voltage source is made with in half cycle and voltage is restored almost instantly with freezed synchronizing template such that operation of DGs are not distributed, and they share the load as per their rating as 17 KW and 10.5 KVAR, 18.2 KW and 11.8 KVAR and 10.2 KW and 7.05 KVAR from DG1, DG2 and DG3 respectively, maintaining sinusoidal current wave shape (refer Fig 4.9). At t=0.2s load is decreased to 30.5 KW and 17.7 KVAR to match the local generation by DGs. The power is accordingly shared as 12.5 KW and 7.03 KVAR, 12.5 KW and 7.45 KVAR and 6.85 KW and 4.44 KVAR between DG1, DG2 and DG3. It may be observed that the capacity of DG1 is not breached even if it is acting as a voltage source. When at t=0.3s DG3 fails, its capacity is then shared between DG1 and DG2 as 15.3 KW and 8.9 KVAR and 16 KW and 9.7 KVAR respectively by ensuring that capacity of DG1 is never breached. In Fig 4.10 it may be observed that DG2 has shared the load greater than the corresponding ratio.

4.4 Performance evaluation of new coupled DG based microgrid for enhanced reliability:

Fig.4.11 depicts the model of considered microgrid which is connected to mains through a Static Transfer Switch (STS). The micro grid comprises of three DG's as before (VSC-1 of DG1, DG2 & DG3), a STATCOM (VSC-0 of DG1) and local RL load, connected parallel through a single distributed line. The DG's comprised of micro sources is represented by a, the VSC with battery support which connect the dc micro source to the distribution system. VSC-0 is considered to act as master in islanded mode. The DG sources are invariably configured to work as current source adding current to each node in phase with voltage at PCC, thereby dealing only with real power. The VSC-0 acts as STATCOM in grid connected mode and is operated through indirect current control, thus enable the drawl of only real power from the grid. In order to keep the operation of the STATCOM within safe limits only 30% of the net reactive power is allocated to the STATCOM for compensation in grid connected mode, the rest is distributed among the rest as per their capacities. In the

Islanded mode the voltage template at the grid tied mode is freezed by the PLL which operates the VCO-0, and the control is switched from indirect current control mode to PWM mode making it a voltage source and routing the power from coupled DC bus of the DG1. Table 4.3 depicts parameters of the considered system.

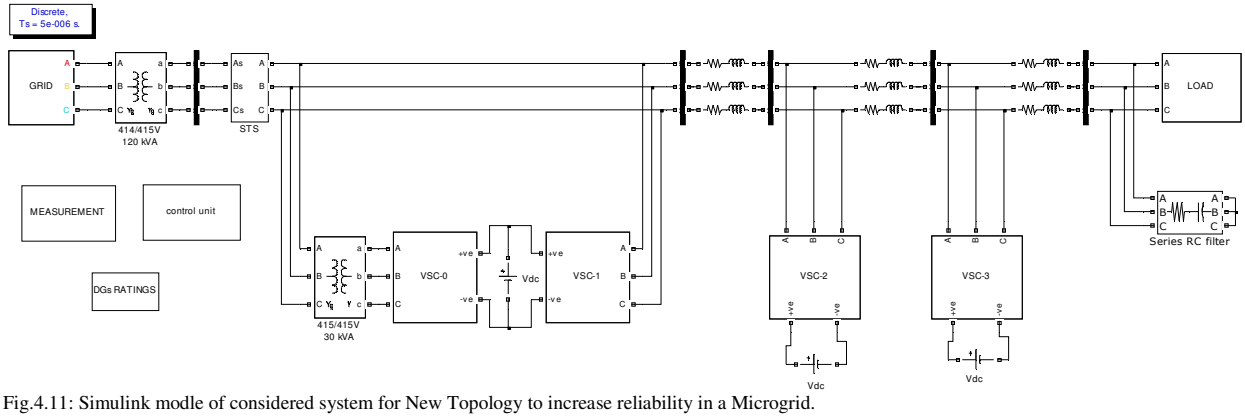

Fig.4.11: Simulink modle of considered system for New Topology to increase reliability in a Microgrid.

TABLE 4.3. PARAMETERS OF THE CONSIDERED SYSTEM COUPLED DG BASED MICROGRID FOR ENHANCED RELIABILITY

DG1 Power Rating	50 KVA
DG2 Power Rating	30 KVA
DG3 Power Rating	20 KVA
Isolated Transformers Power rating	100 KVA
Line Impedance	0.01334 Ω, 0.03 mH
Load	15-100 KVA at 0.8 pf
LCL filter (L_{f1}, C_f, L_{f2})	1.5 mH, 15 µF, 0.5 mH
Passive filter (RC)	1Ω, 100µF
Passive filter	1µF
DC Voltage (Each DG)	800v

The performance of the system is studied under three cases

Case 1:

The mains is considered supplying constant power of 26.5 KW to the microgrid, and the balance power is supplied by the active DG's in the microgrid. It may be observed from Fig 4.13, that initial load demand of 68 KW and 25.2 KVAR is catered by mains which contributes 26.5KW, and the remaining load demand is contributed by DG's depending upon their ratings as 6.5 KW and 11.2 KVAR and 18.5 KW and 8.3 KVAR, 12.7 KW and 5.8 KVAR and 8.5 KW and 4.1 KVAR respectively from VSC-0 and VSC-1 of DG1, DG2 and DG3(including microgrid losses). It may also observe that current drawl from the mains is at unity power factor where current is shown to be in phase with the voltage. From Fig 4.13 it may be observed that, the transients due to disturbances like load perturbations, DG failures

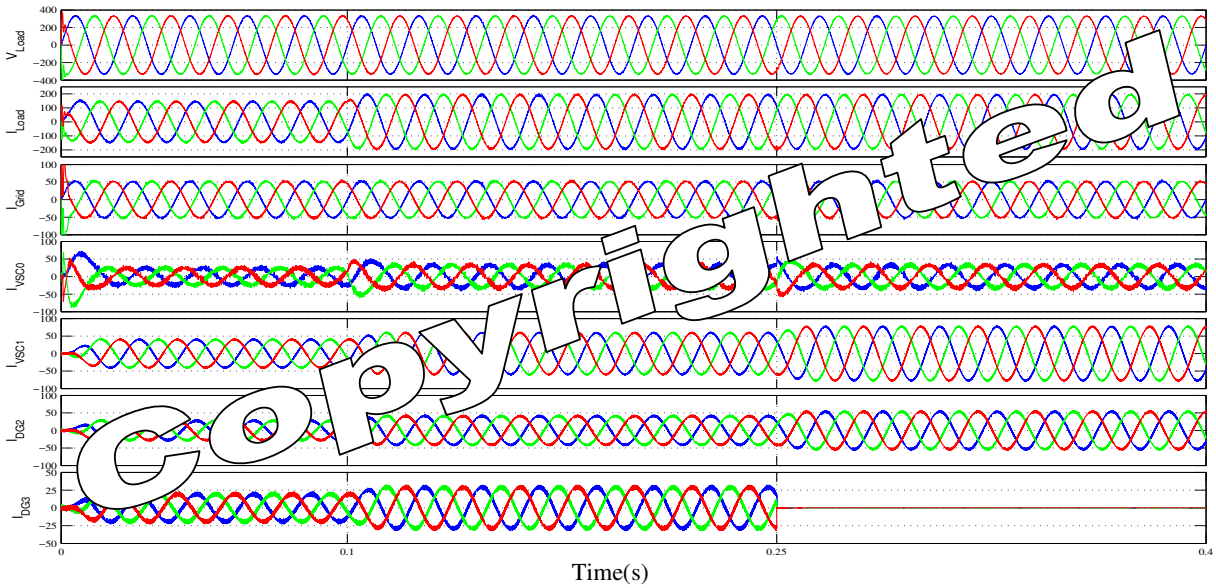

Fig 4.12: Current and Voltage wave forms of Microgrid under Grid connected mode (case 1)

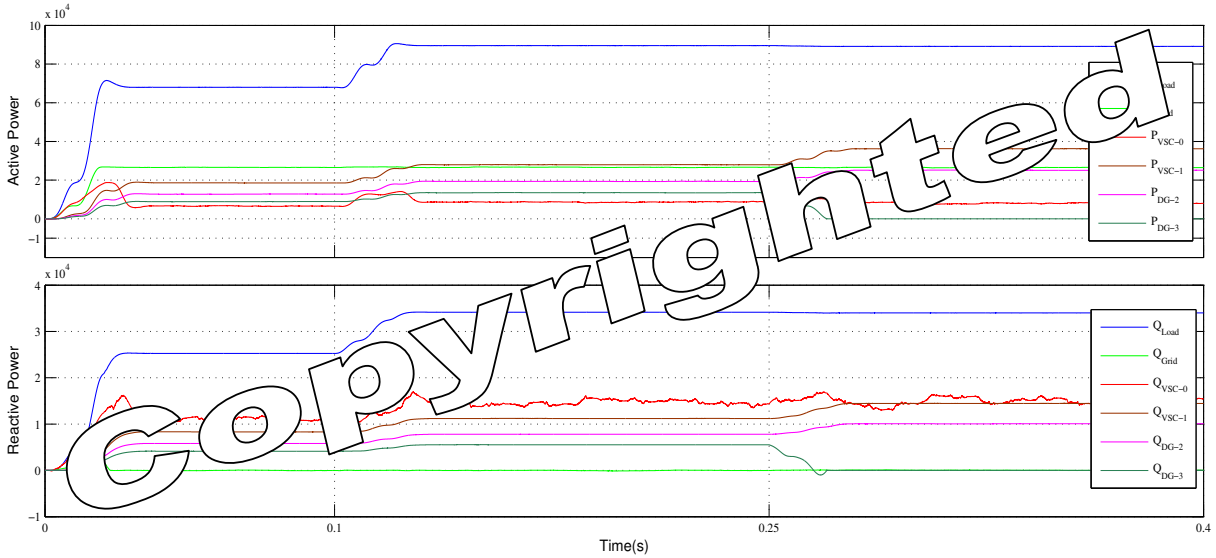

Fig 4.13: Active and Reactive Power wave forms of Microgrid under Grid connected mode (case 1)

ect. is taken care by the VSC-0 of DG1. Starting at t=0, during the transient period the active and reactive power contribution by DG1 is increased from 0 KW to 18.7 KW and 0 KVAR to 16.2 KVAR, and after the transient period the active and reactive power contribution of VSC-0 of DG1 is settled to 6.5 KW and 11.2 KVAR. When at t=0.1s the load is increased to 89.5 KW and 34.1 KVAR, the increased demand is supplied by the active DG's in the system depending upon their ratings as 27.9 KW and 11.2 KVAR, 19.3 KW and 7.8 KVAR and 13.5 KW and 5.5 KVAR respectively from DG1, DG2 and DG3. Where as the main's contribution remains constant. During transient period the active and reactive power contribution of VSC-

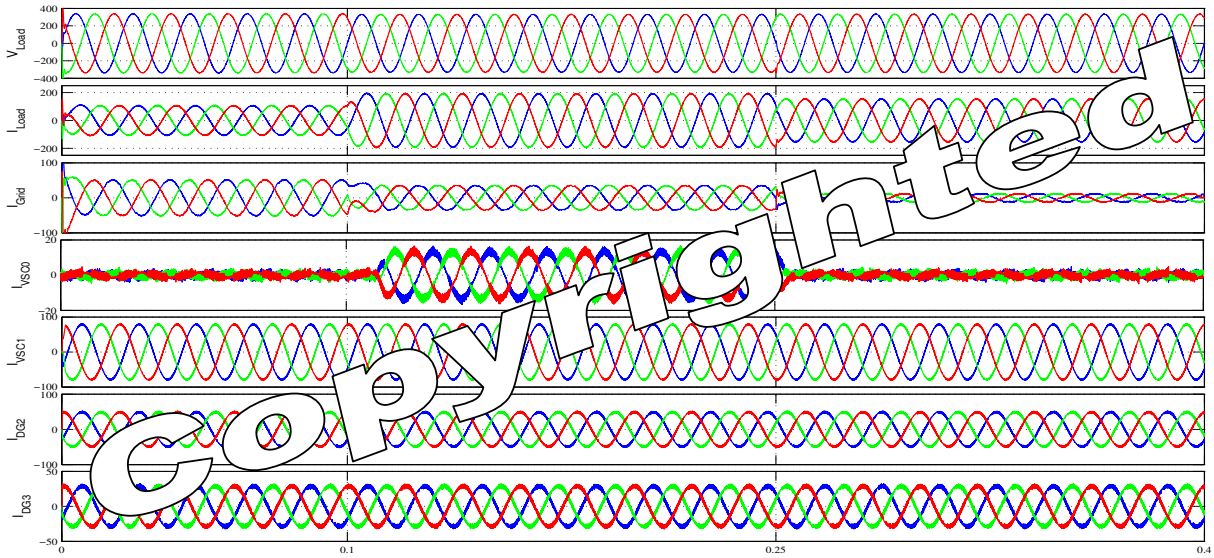

Fig 4.14: Current and Voltage wave forms of Microgrid under Grid connected mode (case 2)

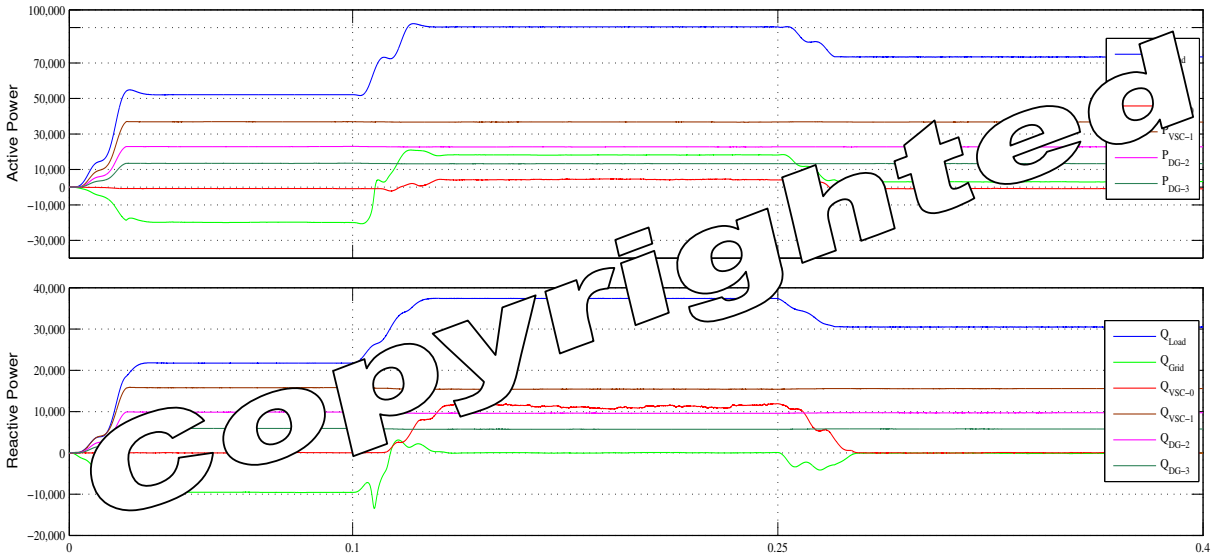

Fig 4.15: Active and Reactive Power wave forms of Microgrid under Grid connected mode (case 2)

0 of DG1 is increased from 6.5 KW to 14.1 KW and 11.2 KVAR to 17 KVAR, and after the transient period the active and reactive power contribution by VSC-0 is settled to 8.5 KW and 14 KVAR. At t=0.25 sec, DG3 fails, ultimately making the current I_{DG-3} =0, its share of power is then contributed by other DG's depending upon their ratings as 36.2 KW and 14.4 KVAR and 25.1 KW and 10 KVAR respectively from DG1 and DG2. The transient here also contributed by VSC-0, During transient period the active and reactive power peak takes 10.98 KW and 16.9 KVAR, and after the transient period the active and reactive power contribution by mains is settled to 7.8 KW and 14.4 KVAR.

Case 2:

The DGs is considered supplying constant power of 36.8 KW and 15.8 KVAR, 22.85 KW and 9.85 KVAR and 13.4 KW and 5.9 KVAR respectively from VSC-1 of DG1, DG2 and DG3. The supply-demand balance is purely taken care by the grid and VSC-0 of DG1. It may be observed from Fig 4.15, that initial load demand of 52.1 KW and 21.7 KVAR whereas the DGs generation is 73 KW and 31.55 KVAR, the surplus generation is fed back to the grid. When at t=0.1s the load is increased to 90.4 KW and 37.4 KVAR, whereas the DGs still generate 73 KW and 31.55 KVA, the deficit active power is supplied by the grid and the deficit reactive power is supplied by the VSC-0. At t=0.25 sec, the load demand is 73 KW and 30.45 KVAR which is almost equal to the generation by all DGs then the grid supplies a very small current just enough to maintain the voltage.

Case 3:

Control of DGs become critical while its operation in islanded mode amidst their limited capacities. It is therefore load corresponding to sum of capacities of slave DGs and 50% capacity of master DG is kept in the Islanded microgrid and remaining non critical load is shedded. The shedding of the non-critical load is done in a chunk as soon as islanded condition is detected. Fig 4.17 depicts the microgrid response to load perturbations and failure of DG3 from the microgrid. From t=0s to t=0.1s the grid connected operation is considered, accordingly connected load of 88.3 KW and 33.64 KVAR is supported. The contribution of mains remains of 26.5 KW and remaining power is shared by DG's as per their ratings as 8.8 KW and 15 KVAR and 27.43 KW and 11.05 KVAR, 18.95 KW and 7.7 KVAR and 13.15 KW and 5.45 KVAR respectively from VSC-0 and VSC-1 of DG1, DG2 and DG3 (including microgrid losses). At t=0.1s it may be observed that microgrid is islanded from mains and connected load is reduced to 31.8 KW and 10.25 KVAR. It may further be observed that distortion due to switching is now present due to VSC-0 of DG1 taking over as a voltage source. It may also be clear that transition of VSC-0 from current source to voltage source is made with in half cycle and system voltage is restored almost instantly with freezed synchronizing template such that operation of DGs are not distributed, and they share the load as per their rating as 14 KW and 4.75 KVAR, 9.5 KW and 3.3 KVAR and 6.5 KW and 2.35 KVAR from DG1, DG2 and DG3 respectively, maintaining sinusoidal current wave shape (refer Fig 4.16). At t=0.2s load is increased to 54.75 KW and 19.7 KVAR. The power is accordingly shared as 25KW and 9.1 KVAR, 17 KW and 6.3 KVAR and 11.8 KW and 4.5 KVAR between DG1, DG2 and DG3. As explained before in grid connected mode, here also the transient was taken care by VSC-0 of DG1, its contribution is

increased from 2.3 KW to 8.6 KW and 0 KVAR to 2.9 KVAR. After the transient period its contribution is settled back to2.3 KW and 0 KVAR. When at t=0.3s DG3 fails, its capacity is shared between DG1 and DG2 as 33.4 KW and 11.9 KVAR and 22.1 KW and 8.2 KVAR respectively by ensuring that capacity of DG1 is never breached.

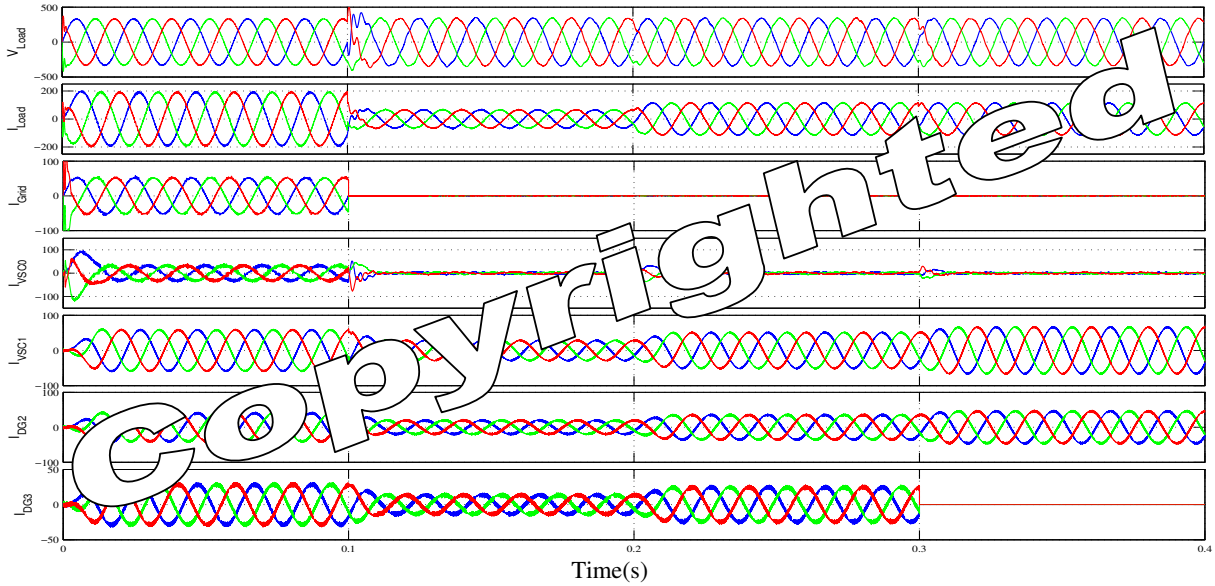

Fig 4.16: Current and Voltage wave forms of Microgrid under Islanded mode

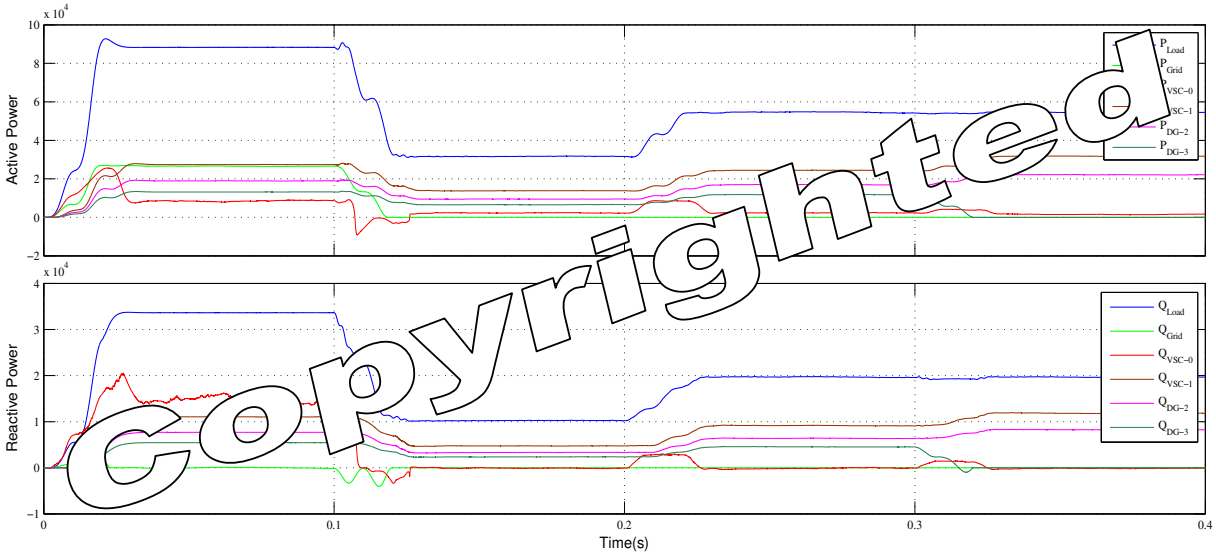

Fig 4.17: Active and Reactive Power wave forms of Microgrid under Islanded mode

CHAPTER-5

Main Conclusion and Future Scope of Work

5.1 General:

Inclusion of DGS in the grid to form a micro grid is a popular research area and requisite future need. For efficient and fast interface with ac grid, current controlled grid coupling is advocated. The flexibility provided by the said control include fast coupling and decoupling, fast absorption of transients, auto protection of DGs due to current limiting feature, easy incorporation of PQ improvement feature, optimal utilization of the capacity of VSC, better co-operation between DGs and possible up gradation of control scheme to smart grid applications. The present chapter summaries the investigations carried out and accordingly main conclusion are derived and suggestions for further work are also presented.

5.2 Main Conclusion:

The MATLAB / Simulink environment using SimPower systems block set has been used to develop the model and carry out simulation work. Master slave configuration has been adopted in islanded mode, otherwise all DGs acts as current controlled sources. The current controlled DGs for micro grid offer several advantages over voltage controlled DGs. The study conducted and reported in the thesis clearly state the advantages of fast, flexible and efficient control of DGs over the reported control of voltage source converter.

Two distinctly new control strategies, one based on centralized control, which require inter communication for control parameters and other that deals with independent control of DGs by sensing the voltage and current at its PCC are discussed , and validated by simulation results. The centralized control too offers sensor reduction, while independent control guarantee fast control and good coordination amongst DGs. These scheme drive the DGs to share the loads based on their capacitor and handles the transients effectively so that the same is not reflected in the mains. In addition the drawl from the mains is done above 0.9 Pf at the all the time.

A fast transition from grid control mode to off grid mode is also demonstrated by simulation results. The DG corresponding to highest rating is connected from current controlled mode to islanded mode as “Master”, which marks the voltage of the micro grid, a share only a load fraction of its capacity to effectively absorb transients on the micro grid and maintain the stability. The presented results reveal that DG corresponding to Master has never breached the

capacity limit and easily handled the power matching in cohesion with other DGs for both the control schemes. Variety of dynamics has been presented through results, which may include load parameters and DGs moving into / out from the micro grid. The results demonstrate that both schemes have shown fast response in handling load sharing and transients, besides regulating the current from the mains in grid connected mode and supporting the master in islanded mode. In a new configuration presented the master DG couple with another slave DG directly connected to the grid to patch the power requisite by the master for un-warranted circumstances. A bidirectional power flow through the DG bus coupling make the master versatile and capable of supporting even without battery storage.

5.3 Future Scope of Work:

The presented control schemes pave the way for variety of additional scope to the presented work. For instance the scheme can be modified to provide compensation to PQ problems on the micro grid hence can effectively utilize the capacity of the VSC, and reduces the cross coupling of DGs for reactive power, harmonics and negative sequence currents. The inherent quality of the scheme may be utilized in the work for developing and integrating the protection system, since the control algorithm provides the facility to auto protect the hardware and provide sufficient time for the protection system to operate without interruptions judiciously. The DGs in current control particularly the renewable energy systems which have variable power output, and fluctuates over a large range with faster dynamics. Studies may be conducted to include these variable sources for dynamic equalization. Since the dealt control schemes offer high degree of flexibility, the studies may be conducted in the assessment of placement of storage system/ independent on RES. Above all hardware implementation on small scale incorporating the RES, storage element and VSCs in proposed configuration with both control schemes may be done.

REFERENCES

[1] S. Chowdhury, S.P. Chowdhury and P. Crossley, "Microgrids and Active Distribution Networks".

[2] Robert Lasseter, Abbas Akhil, Chris Marnay, John Stephens, Jeff Dagle, Ross Guttromson, A. Sakis Meliopoulous, Robert Yinger, and Joe Eto "White Paper on Integration of Distributed Energy Resources: The CERTS Micro Grid Concept," April, 2002.

[3] Veda Prakash Galigekere and Marian K. Kazimierczuk, "ROLE OF POWER ELECTRONICS IN RENEWABLE ENERGY SYSTEMS".

[4] Frede Blaabjerg, Zhe Chen,and Soren Baekhoej Kjaer, "Power Electronics as Efficient Interface in Dispersed Power Generation Systems," IEEE Trans. Power Electron.,vol. 19, no. 5, pp. 1184-1194, Sep. 2004.

[5] Geoferry R. Walker, Paul C. Sernia, " Cascaded DCDC Converter Connection of Photovoltaic Modules", IEEE Trans. Power, Electron., vol. 19, pp. 1130-1139, July 2004.

[6] J. P. Pinto, R. Pregitzer, L. F. C. Monteiro, and J. L. Afonso, "3-phase 4-wire shunt active power filter with renewable energy interface," presented at the Conf. IEEE Rnewable Energy & Power Quality, Seville, Spain, 2007.

[7] M. Kazmierkowski, R. Krishnan, and F. Blaabjerg, Control in Power Electronics—Selected Problems. New York: Academic, 2002.

[8] J. Svensson, "Synchronisation methods for grid-connected voltage source converters," Proc. Inst. Electr. Eng.—Gener. Transm. Distrib., vol. 148, no. 3, pp. 229–235, May 2001.

[9] H. Kim, S.-J. Lee, and S.-K. Sul, "Reference wave generator in dynamic voltage restorers by use of PQR power theory," in Proc. IEEE APEC, 2004, vol. 3, pp. 1452–1457.

[10] S.-J. Lee, H. Kim, S.-K. Sul, and F. Blaabjerg, "A novel control algorithm for static series compensators by use of PQR instantaneous power theory," IEEE Trans. Power Electron., vol. 19, no. 3, pp. 814–827, May 2004.

[11] R. Teodorescu, F. Iov, and F. Blaabjerg, "Flexible development and test system for 11 kW wind turbine," in Proc. IEEE PESC, 2003, vol. 1, pp. 67–72.

[12] E. Twining and D. G. Holmes, “Grid current regulation of a three-phase voltage source inverter with an LCL input filter,” IEEE Trans. Power Electron., vol. 18, no. 3, pp. 888–895, May 2003.

[13] S. Fukuda and T. Yoda, “A novel current-tracking method for active filters based on a sinusoidal internal model,” IEEE Trans. Ind. Electron., vol. 37, no. 3, pp. 888–895, 2001.

[14] X. Yuan, W. Merk, H. Stemmler, and J. Allmeling, “Stationary-frame generalized integrators for current control of active power filters with zero steady-state error for current harmonics of concern under unbalanced and distorted operating conditions,” IEEE Trans. Ind. Appl., vol. 38, no. 2, pp. 523–532, Mar./Apr. 2002.

[15] R. Teodorescu and F. Blaabjerg, “Proportional-resonant controllers. A new breed of controllers suitable for grid-connected voltage-source converters,” in Proc. OPTIM, 2004, vol. 3, pp. 9–14.

[16] D. Zmood and D. G. Holmes, “Stationary frame current regulation of PWM inverters with zero steady-state error,” IEEE Trans. Power Electron., vol. 18, no. 3, pp. 814–822, May 2003.

[17] F. Blaabjerg, R. Teodorescu, M. Liserre, and A. V. Timbus, “Overview of control and grid synchronization for distributed power generation systems,” IEEE Trans. Ind. Electron., vol. 53, no. 5, pp. 1398–1409, Oct. 2006.

[18] J. Svensson, “Synchronisation methods for grid-connected voltage source converters,” Proc. Inst. Elect. Eng., vol. 148, no. 3, pp. 229–235, May 2001.

[19] M. Karimi-Ghartemani and M. Iravani, “A method for synchronization of power electronic converters in polluted and variable-frequency environments,” IEEE Trans. Power Syst., vol. 19, no. 3, pp. 1263–1270, Aug. 2004.

[20] Yazdani, D.; Bakhshai, A.; Joos, G.; Mojiri, M., “A Nonlinear Adaptive Synchronization Technique for Grid-Connected Distributed Energy Sources,” IEEE Trans. Power Electron., vol.23, pp. 2181-2186, July 2008.

[21] P. Mahat, Z. Chen, and B. Bak-Jensen, “Review of islanding detection methods for distributed generation,” in Proc. 3rd Int. Conf. Electric Utility Deregulation and Restructuring and Power Technologies, Apr. 6–9, 2008, pp. 2743–2748.

[22] R. A. Walling, and N. W. Miller, “Distributed generation islanding implications on power system dynamic performance,” IEEE Power Engineering Society Summer Meeting, vol.1, pp. 92-96, 2002.

[23] A. Greenwood, Electrical Transients in Power Systems, New York: Wiley, 1971, pp. 83.

[24] M. A. Refern, O. Usta, and G. Fielding, "Protection against loss of utility grid supply for a dispersed storage and generation unit," IEEE Transaction on Power Delivery, vol. 8, no. 3, pp. 948-954, July 1993.

[25] M. Ropp, K. Aaker, J. Haigh, and N. Sabhah, "Using Power Line Carrier Communications to Prevent Islanding," in Proc. 28th IEEE Photovoltaic Specialist Conference, pp. 1675-1678, 2000.

[26] M. A. Redfern, J. I. Barren, and O. Usta, "A new microprocessor based islanding protection algorithm for dispersed storage and generation units," IEEE Trans. Power Delivery, vol. 10, no. 3, pp. 1249-1254, July 1995.

[27] J. Warin, and W. H. Allen, "Loss of mains protection," in Proc. 1990 ERA Conference on Circuit Protection for industrial and Commercial Installation, London, UK, pp. 4.3.1-12.

[28] F. Pai, and S. Huang, "A detection algorithm for islanding-prevention of dispersed consumer-owned storage and generating units," IEEE Trans. Energy Conversion, vol. 16, no. 4, pp. 346-351, 2001.

[29] P. O'Kane, and B. Fox, "Loss of mains detection for embedded generation by system impedance monitoring," in Proc. Sixth International Conference on Developments in Power System Protection, pp. 95-98, March 1997.

[30] S. I. Jang, and K. H. Kim, "An islanding detection method for distributed generations using voltage unbalance and total harmonic distortion of current," IEEE Tran. Power Delivery, vol. 19, no. 2, pp. 745-752, April 2004.

[31] S. Jang, and K. Kim, "Development of a logical rule-based islanding detection method for distributed resources," in Proc. IEEE Power Engineering Society Winter Meeting, vol. 2, pp. 800-806, 2002.

[32] H. Kabayashi, K. Takigawa, and E. Hashimato, "Method for preventing islanding phenomenon on utility grid with a number of small scale PV systems," Second IEEE Photovoltaic Specialists Conference, vol.1, pp. 695-700, 1991.

[33] J. E. Kim, and J. S. Hwang, "Islanding detection method of distributed generation units connected to power distribution system," in Proc. 2000 IEEE Power System Technology Conference, pp. 643-647.

[34] G. A. Smith, P. A. Onions, and D. G. Infield, "Predicting islanding operation of grid connected PV inverters," IEE Proc. Electric Power Applications, vol. 147, pp. 1-6, Jan. 2000.

[35] M. E. Ropp, M. Begovic, A. Rohatgi, G. Kern, and R. Bonn, "Determining the relative effectiveness of islanding detection methods using phase criteria and non-detection zones," IEEE Transaction on Energy Conversion, vol. 15, no. 3, pp. 290-296, Sept. 2000.

[36] M. E. Ropp, M. Begovic, and A. Rohatgi, "Analysis and performance assessment of the active frequency drift method of islanding prevention," IEEE Tran. Energy Conversion, vol. 14, no 3, pp. 810-816, Sep. 1999.

[37] V. Menon, and M. H. Nehrir, "A hybrid islanding detection technique using voltage unbalance and frequency set point," IEEE Tran. Power Systems, vol. 22, no. 1, pp. 442-448, Feb. 2007.

[38] J. Yin, L. Chang, and C. Diduch, "A new hybrid anti-islanding algorithm in grid connected three-phase inverter system," 2006 IEEE Power Electronics Specialists Conference, pp. 1-7.

[39] A. Tuladhar, Advanced Control Techniques for Parallel Inverter Operation Without Control Interconnections, Dept of Electrical and Computer Engineering, The University of British Columbia, 2000.

[40] R. Majumder, et al., Load sharing with parallel inverters in distributed generation and power system stability, in: Smart Systems 2007 "Technology, Systems and Innovation", 2007.

[41] J.-F. Chen, C.-L. Chu, Combination voltage-controlled and current-controlled PWM inverters for UPS parallel operation, IEEE Transactions on Power Electronics 10 (5) (1995) 547–558.

[42] J.-F. Chen, C.-L. Chu, Y.-C. Lieu, Modular parallel three-phase inverter system, in: Proceedings of the IEEE International Symposium on Industrial Electronics, 1995.

[43] J.P. Lopes, MICROGRIDS Large Scale Integration of Microgeneration to Low Voltage Grids-Emergency Strategies and Algorithms, 2004.

[44] M. Prodanovic, T.C. Green, High-quality power generation through distributed control of a power park microgrid, IEEE Transactions on Industrial Electronics 53 (October (5)) (2006) 1471–1482.

[45] T.C. Green, M. Prodanovic, Control of inverter-based micro-grids, Electric Power Systems Research 77 (9) (2007) 1204–1213.

[46] D.J. Perreault, J.G. Kassakian, Distributed interleaving of paralleled power converters, IEEE Transactions on Circuits and Systems 44 (8) (1997) 728–734.

[47] D.J. Perreault, K. Sato, R.L. Selders, J.G. Kassakian, Switching-ripple-based current sharing for paralleled power converters, IEEE Transactions on Circuits and Systems 46 (10) (1999) 1264–1274.

[48] H. Hanaoka, M. Nagai, M. Yanagisawa, Development of a novel parallel redundant UPS, in: The 25th International Telecommunications Energy Conference, 2003.

[49] K.-H. Kim, D.-S. Hyun, A high performance DSP voltage controller with PWM synchronization for parallel operation of UPS systems, in: 37th IEEE Power Electronics Specialists Conference, 2006.

[50] S. Tamai, M. Kinoshita, Parallel operation of digital controlled UPS system, in: International Conference on Industrial Electronics, Control and Instrumentation, 1991.

[51] Z. Qinglin, C. Zhongying, W. Weiyang, Improved control for parallel inverter with current-sharing control scheme, in: CES/IEEE 5th International Power Electronics and Motion Control Conference, 2006.

[52] Y. Xing, L.P. Huang, Y.G. Yan, A decoupling control method for inverters in parallel operation, in: International Conference on Power System Technology, PowerCon 2002, 2002.

[53] C.-C. Hua, K.-A.L., J.-R. Lin, Parallel operation of inverters for distributed photovoltaic power supply system, in: IEEE Annual Power Electronics Specialists Conference.

[54] M.C. Chandorkar, D.M. Divan, R. Adapa, Control of parallel connected inverters in standalone AC supply systems, IEEE Transactions on Industry Applications 29 (1) (1993).

[55] I. Takahashi, T. Noguchi, A new quick-response and high-efficiency control strategy of an induction motor, IEEE Transactions on Industry Applications IA (22) (1986) 820–827.

[56] M.C. Chandorkar, D.M. Divan, B. Banerjee, Control of distributed ups systems, in: IEEE Annual Power Electronics Specialists Conference, 1994.

[57] C.K. Sao, P.W. Lehn, Autonomous load sharing of voltage source converters, IEEE Transactions on Power Delivery 20 (2) (2005) 1009–1016.

[58] M. Xie, YL, K. Cai, P. Wang, X. Sheng, A novel controller for parallel operation of inverters based on decomposing of output current, in: Industry Applications Conference 2005: Conference Record of the 2005 Fortieth IAS Annual Meeting, 2005.

[59] A. Engler, Control of parallel operating battery inverters, in: Photovoltaic Hybrid Power Systems Conference, Aix-en-Provence, 2000.

[60] A. Engler, M. Meinh, M. Rothert, New V/f-statics controlled battery inverter: Sunny Island—the key component for AC-coupled hybrid systems and mini grids, in: 2nd European PV Hybrid and Mini-Grid Conference, Kassel, 2003.

[61] A. Engler, et al., Pure AC-coupling —the concept for simplified design of scalable PV-hybrid systems using voltage/frequency statics controlled battery inverters, in: 14th International Photovoltaic Science and Engineering Conference (PVSEC-14), Bangkok, 2004.

[62] A. Engler, Applicability of droops in low voltage grids, in: 3rd European PVHybrid and Mini-Grid Conference, Aix-en-Provence, France, 2006.

[63] P. Karlsson, J. Björnstedt, M. Ström, Stability of voltage and frequency control in distributed generation based on parallel-connected converters feeding constant power loads, in: EPE, Dresden, Germany, 2005.

[64] A. Engler, N. Soultanis, Droop control in LV-grids, in: International Conference Future Power Systems, Amsterdam, Niederlande, 2005.

[65] A. Engler, Applicability of droops in low voltage grids, International Journal of Distributed Energy Resources 1 (1) (2005).

[66] R.H. Lasseter, MicroGrids, in: Power Engineering Society Winter Meeting, 2002.

[67] R. Lasseter, P. Piagi, Control and Design of Microgrid Components, University of Wisconsin-Madison, 2006, P.P. 06-03.

[68] R.H. Lasseter, Microgrids and distributed generation, Journal of Energy Engineering (2007).

[69] M. Brucoli, T.C. Green, Fault response of inverter dominated microgrids, in: 2nd International Conference on Integration of Renewable and Distributed Energy Resources, Napa, CA, USA, 2006.

[70] J.M. Guerrero, et al., Drop control method for the parallel operation of online uninterruptible power systems using resistive output impedance, in: Applied Power Electronics Conference and Exposition, 2006: APEC'06, Twenty-First Annual IEEE, 2006.

[71] J.M. Guerrero, et al., A wireless controller to enhance dynamic performance of parallel inverters in distributed generation systems, IEEE Transactions on Power Electronics 19 (5) (2004) 1205–1212.

[72] J.M. Guerrero, et al., A wireless controller for parallel inverters in distributed online UPS systems, in: The 29th Annual Conference of the IEEE Industrial Electronics Society, 2003.

[73] J.M. Guerrero, J. Matas, L.G. de Vicuna, N. Berbel, J. Sosa, Wireless-control strategy for parallel operation of distributed generation inverters, in: Industrial Electronics, 2005, ISIE 2005, 2005.

[74] J.M. Guerrero, N. Berbel, J. Matas, L.G. de Vicuna, J. Miret, Decentralized control for parallel operation of distributed generation inverters in microgrids using resistive output impedance, in: 32nd Annual Conference on IEEE Industrial Electronics, IECON 2006, Paris, France, 2006.

[75] J.M. Guerrero, J. Matas, L.G. De Vicuna, M. Castilla, J. Miret, Wireless-control strategy for parallel operation of distributed-generation inverters, IEEE Transactions on Industrial Electronics 53 (5) (2006) 1461–1470.

[76] J.M. Guerrero, et al., Control of line-interactive UPS connected in parallel forming a microgrid, in: IEEE International Symposium on Industrial Electronics, Vigo, Spain, 2007.

[77] J.M. Guerrero, et al., Parallel operation of uninterruptible power supply systems in MicroGrids, in: EPE 2007, Aalborg, Denmark, 2007.

[78] K.D. Brabandere, et al., A voltage and frequency droop control method for parallel inverters, in: The 35th IEEE PESC Conference, Aachen, Germany, 2004.

[79] K. De Brabandere, et al., Prevention of inverter voltage tripping in high density PV grids, in: 19th EU-PVSEC, Paris, France, 2004.

[80] K. De Brabandere, et al., Control of microgrids, in: IEEE Power Engineering Society General Meeting, Tampa, FL, 2007.

[81] L. Mihalache, Paralleling control technique with no intercommunication signals for resonant controller-based inverters, in: 38th IAS Annual Meeting Industry Applications Conference, 2003.

[82] S.J. Chiang, J.M. Chang, Parallel control of the ups inverters with frequencydependent drop scheme, in: IEEE 32nd Annual Power Electronics Specialists Conference, 2001, PESC Record.

[83] H.-C. Chiang, A frequency-dependent droop scheme for parallel control of UPS inverters, Journal of Chinese Institute of Engineers 24 (2001) 699–708.

[84] M.N. Marwali, J.-W. Jung, A. Keyhani, Control of distributed generation systems. Part II. Load sharing control, IEEE Transactions on Power Electronics 19 (6) (2004).

[85] H.-P. Glauser, et al., New inverter module with digital control for parallel operation, in: The Third International Telecommunications Energy Special Conference, 2000.

[86] X. Chen, Y. Kang, J. Chen, Operation, control technique of parallel connected high power three-phase inverters, in: The 4th International Power Electronics and Motion Control Conference, 2004.

[87] Ali Keyhani Mohammad N, Marwali Min Dai, "Integration of Green and Renewable Energy in Electric Power Systems".

[88] P. Rodríguez, J. Pou, J. Bergas, I. Candela, R. Burgos and D. Boroyevich, "Double Synchronous Reference Frame PLL for Power Converters Control".